

Drew University College of Liberal Arts

Demystifying the Atmosphere with a Model Aerosol System:
The Photo-enhanced Ozonolysis of Surface Adsorbed Organics

A Thesis in Chemistry

by

Alae Z. Kawam

Submitted in Partial Fulfillment of the Requirements for the Degree of Bachelor in Arts

With Specialized Honors in Chemistry

May 2014

Abstract	4
Chapter 1: Introduction	5
1.1 The Structure and Components of the Atmosphere Determine Its Chemistry	6
1.2 Gas-Solid Interface Chemistry is Known as Heterogeneous Chemistry	7
Formation of aerosols	7
Why is Heterogeneous chemistry important?	9
1.3 Photochemistry in the atmosphere	13
Formation of tropospheric oxidants via photochemical processes	18
1.4 Aerosols, Natural and Anthropogenic, are Ubiquitous in the Atmosphere	20
1.5 Biomass Combustion Releases Methoxyphenols and other Compounds	21
1.6 Chemical Diversity is Common on Single Substrates	24
1.7 Aerosol's Role in Climate Change is Associated with Uncertainty	25
1.8 Modeling Adsorbed Lignin Pyrolysis Product Reactions Requires Atmospheric Relevance	28
1.9 Designing a Representative Atmospheric Model to Obtain Quantitative Information	30
Chapter 2: Kinetic Experimental Methods	34
2.1 Why Study Reaction Kinetics?	34
2.2 What are Reaction Kinetics?	35
2.3 How was Kinetic Data Obtained?	35
2.5 Experimental Setup	40
2.6 An Introduction to NMR	42
2.7 Experimental Techniques for NMR	44
2.8 An Introduction to GC-MS	45
2.9 GC-MS Specifications and Techniques	46
Chapter 3: Vanillin Kinetic Studies	47
3.1 Identification of Functional Groups on IR Spectra	47
3.2 Identification of Ozonolysis Products	49
3.3 Kinetic Analysis of DRIFTS Data	53
3.4 Preliminary Analysis of Photoenhanced Vanillin Ozonolysis	57

3.5 Modeling Kinetic Data	58
3.6 Kinetic Analysis is Used to Determine the Mechanism of Ozonolysis of Vanillin	64
Chapter 4: Eugenol Kinetic Studies	67
4.1 Preliminary Analysis	68
4.2 A deeper look into Eugenol Ozonolysis Kinetics	72
4.3 Product Identification via GC-MS and NMR	74
Chapter 5: Importance of Heterogeneous and Photo-enhanced Chemistry in the Troposphere	76

Abstract

The chemical behavior of atmospheric aerosols is an area of great uncertainty due to their diverse chemical composition, unknown reactivity with tropospheric pollutants, and influences of solar radiation. In this study we focus on understanding the influences of simulated solar radiation on biomass burning aerosols by using a laboratory model. We used potassium chloride, a biomass burning tracer, as our solid substrate coated via gas phase adsorption with either eugenol or vanillin as our model semi-volatile lignin pyrolysis products. We used DRIFTS to analyze the reaction kinetics with ozone of these adsorbed organics under light and dark conditions. We identified vanillic acid as the major product of vanillin ozonolysis and homovanillic acid as the major product of eugenol ozonolysis. Ring cleavage products were not directly observed but are inferred by kinetic analysis. Ozonolysis of adsorbed vanillin follows the Langmuir-Hinshelwood mechanism in which ozone partitions to the adsorbed phase and subsequently reacts with vanillin. The maximal rate constant, k_{max} , for this reaction in dark and light were determined to be 0.013 min^{-1} and 0.029 min^{-1} with an ozone equilibrium constant K_{O_3} of $1.81 \times 10^{-14} \text{ cm}^3$. The atmospheric lifetime of vanillin for the dark and light are 8.5 hours and 3.8 hours, respectively. Eugenol ozonolysis occurs at two sites that are affected differently by simulated solar radiation; the alkene side chain ozonolysis is unaffected by simulated solar radiation while the cleavage of the aromatic ring is photoenhanced. Rate constants were used to calculate atmospheric lifetimes of eugenol 18.8 hours and 20.4 hours in the light and dark, respectively. The reaction kinetics and mechanism provides us with valuable information to reduce uncertainty associated with the chemistry of biomass burning aerosols.

Chapter 1: Introduction

The atmosphere is a chemically complex system that influences the climate, biosphere and public health. Its chemistry is driven by incoming radiation from the sun and affects the interrelated chemical reactions of the atmosphere and biological systems. The atmosphere's chemistry is further complicated by interactions of different phases such as gas phase mixtures, solid-liquid interfaces, and gas-solid interfaces that are described by unique chemical principles. Gas phase chemistry in the atmosphere is well understood, but the chemistry of the interactions of different phases in the atmosphere such as solid-gas interfaces is an area of great uncertainty. Thus, the unknown role of solid-gas chemistry on the atmosphere, biosphere, and climate invite us to study the chemical principles that drive the chemistry.

One major source of solid-gas interactions are aerosol surfaces. Aerosols by definition are fine particulate matter suspended in the atmosphere. The ubiquity and chemical diversity of aerosols make it nearly impossible to study these systems in totality, thus understanding these interactions necessitates simplification. I describe here a simplified laboratory system designed to model an aerosol system that allows for the deduction of quantitative information. The proposed model simplifies the complex chemical reactions of a specific class of aerosols that are under the influence of simulated solar radiation.

The class of aerosols studied here is emitted from a naturally occurring source, namely biomass burning plumes. The model aerosol was comprised of a major inorganic compound from biomass burning aerosol, solid potassium chloride, coated with representative organic compounds of biomass burning aerosol, vanillin or eugenol. To

model the complex chemistry of these aerosols, we investigated the influence of solar radiation on the reactions of these laboratory model aerosols exposed to gaseous ozone, a major pollutant present in smog. This laboratory model allowed us to better understand and quantify the environmental factors that influence aerosol chemistry. In the following sections of this chapter, I will further develop pertinent information on aerosols and the experimental process.

1.1 The Structure and Components of the Atmosphere Determine Its Chemistry

The atmosphere is comprised of several distinct layers that lie directly above each other. The layers are separated based on the sudden shift in temperature which is driven by thermodynamics and the difference in solar radiation that each layer absorbs. The solar radiation that is absorbed by one layer does not reach the layer below it, thus the chemical reactions that occur vary. The atmospheric layers in order of increasing altitude are: troposphere (0-12 km), stratosphere (20-50 km), mesosphere (60-80 km), and thermosphere (700 km). For this study, only the chemistry relevant to the troposphere is considered because biomass burning aerosols are emitted directly into the troposphere and are involved in the chemical processes there.

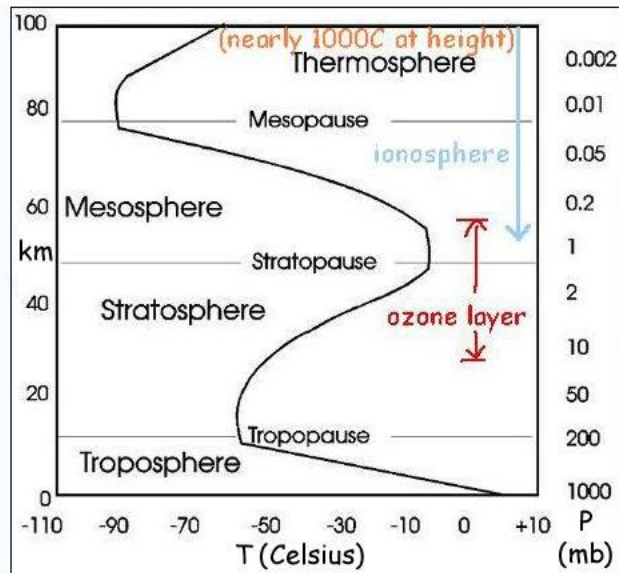


Figure 1.1 : Structure of the atmosphere shows dramatic temperature and pressure changes as a function of altitude (adapted from C.Seligman.)

1.2 Gas-Solid Interface Chemistry is Known as Heterogeneous Chemistry

The study of the chemical interactions specifically between a solid surface and a gas is called heterogeneous chemistry. Because many aerosols are solid particles suspended in a gas, the essence of heterogeneous chemistry is embodied by these fine particles. Gas molecules of different identities can also coat or adsorb onto the solid surface thereby altering its chemical reactivity. Aerosols may also be liquid droplets suspended in air, but the type of chemistry they exhibit is known as multiphase chemistry and is described by different chemical principles. In this section the formation of aerosols, evidence, and significance of aerosols involved in heterogeneous chemistry is explained.

Formation of aerosols

Aerosols can be directly emitted into the atmosphere or may grow on nucleation sites. Atmospheric aerosols change in size by coagulation and gas to particle conversion which requires nucleation sites (Seinfeld and Bessett, 1982) as shown in figure 1.2.

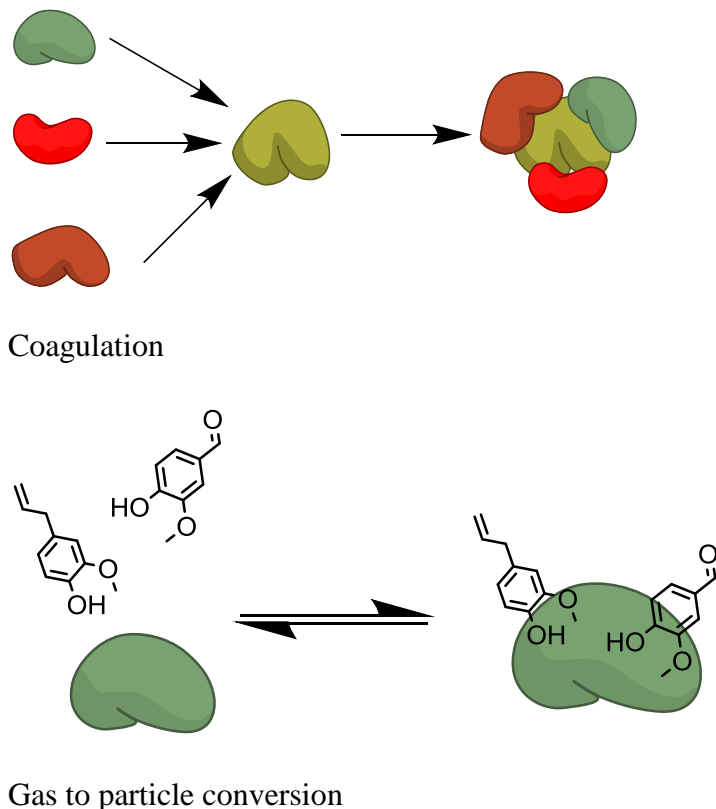


Figure 1.2: Gases can condense to adsorb onto surfaces to make them grow; particles of different composition may also coagulate and form larger particles

There are three mechanisms (or combinations of mechanisms) that control the rate determining step in gas to particle conversion: diffusion controlled (rate of diffusion of the vapor molecule to the surface of the particle), surface reaction controlled (the rate of the surface reaction involving the adsorbed vapor molecule and particle surface) and volume reaction controlled growth (rate of reaction involving aqueous species occurring uniformly throughout the volume of the particle). These mechanisms can be inferred from data on evolution of an aerosol size distribution. By calculating growth rates for

particles of different sizes the functional dependence of growth rate on particle size can be determined (Seinfeld and Bessett, 1982).

Why is heterogeneous chemistry important?

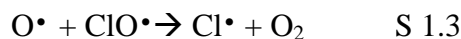
The infamous Antarctic “ozone hole” discovery in which CFCs (chlorofluorocarbons, a chemical used mainly in refrigerants) played a large role in the depletion of the ozone layer was explained through the occurrence of heterogeneous chemistry on stratospheric ice particles. Because CFCs are extremely stable molecules, they pass through the troposphere unchanged and reside in the stratosphere (upper atmosphere) where the ozone layer is located (see figure 1.1). As CFCs absorb ultraviolet radiation, the CFCs dissociate- a chlorine atom is broken off the molecule as shown in Scheme 1.1 (Cicerone, 1975):



This yields a free chlorine atom which removes a single oxygen atom from an ozone molecule forming chlorine monoxide (see S1.2 below)



Free oxygen atoms (which naturally occur in the stratosphere) collide with a chlorine monoxide atom and form O₂ which results in another free chlorine atom.



The cycle of chlorine atoms destroying ozone molecules continues and results in a single chlorine atom’s destruction of numerous ozone molecules. The overall process is shown in S 1.4.



Although the depletion of the ozone layer was known to occur, it was unexplained as to why it occurred so quickly with the onset of the Antarctic spring. The models that used known gas-phase chemistry did not predict the dramatic seasonal loss of ozone. The missing piece was based in heterogeneous chemistry in which a surface catalyzed the reaction. During the winter above Antarctica, a polar vortex develops in the stratosphere. The temperature drops to values as low as 185 K, which allows the small concentration of water (5-6 ppm) to form ice crystals. The air in the vortex remains isolated from other parts of the stratosphere which allows photochemically active products to build up. This sets the stage for ozone destruction when the sun comes up and the polar vortex dissipates. Several Cl reservoir species such as HCl and ClONO₂ occur in the stratosphere slowly regenerate Cl atoms when in the gas phase to destroy ozone. However, on the surfaces of polar stratospheric ice crystals, the reaction occurs very quickly. HCl and ClONO₂ on the surfaces of the ice surfaces normally act as Cl reservoirs but are converted to photochemically active species of Cl₂ and ClNO₂ (nitryl chloride). When the sun comes up in the spring, these species are rapidly photolyzed and generate free chlorine atoms which initiate the ozone destruction chain. The surfaces of polar stratospheric clouds (ice surfaces formed by cold water ice particle condensation) catalyze the reaction (Molina, 1991).

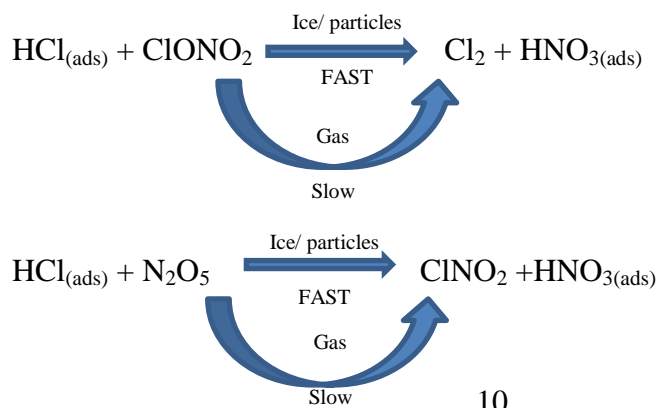
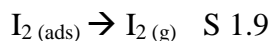
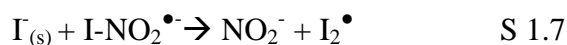
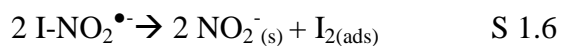


Figure 1.3: Surface catalyzed generation of photo-labile species on polar stratospheric cloud surfaces and become part of the ozone destruction cycle. The reaction in the gas phase occurs much more slowly.

Although the stratospheric ozone is unrelated to this study, this example helps cultivate an appreciation for the significance of heterogeneous chemistry in the atmosphere. The catalytic process of ozone depletion by CFCs had a significant impact on the chemicals used for refrigeration as these compounds were banned (Montreal Protocol, 1987).

Heterogeneous chemistry is also important for determining sources of reactive species in the marine atmospheric boundary layer (it is part of the atmosphere where ocean and atmosphere make direct contact). Halogen species from sea salt particles can be released into the atmosphere. Molecular iodine is an important precursor to particle formation at the marine boundary layer. Although it can originate from biogenic sources such as microalgae and macroalgae, O'Neill and Hinrichs have shown that the heterogeneous chemistry of N_2O_4/NO_2 and sea salt may be a source of nonbiogenic molecular iodine as shown in S 1.5- 1.9 (2011):



The release of nonbiogenic molecular iodine may impact the oxidative capacity of the troposphere. For example, reactive halogen species can catalytically destroy ozone in the marine boundary layer, alter the NO/ NO_2 or OH/ O_2H cycles and can potentially

form ultrafine particulates (Vogt et al., 1999; Read et al., 2008; McFiggins et al., 2000; Saiz-Lopez et al., 2006).

Heterogeneous chemistry is closely associated with catalysis as numerous reactions occur in the presence of a surface that can catalyze chemical reactions. One major example of a heterogeneous reaction is the reactivity of nitrogen dioxide (NO_2), a reddish-brown air pollutant. In the gas phase, NO_2 reacts very slowly and requires an OH or NO_3 radical to initiate a nitration reaction. In the presence of nucleation sites, however, the nitration process occurs (in the presence of low concentrations of HNO_3) and accounts for nitrated organics such as 1-nitropyrene, 2-nitrofluoranthene, and 9-nitroanthracene on particulate matter in suburban areas (the parent compounds are polycyclic aromatic hydrocarbons which result from incomplete combustion of coal, oil, or gas) (Ringuet et al., 2012).

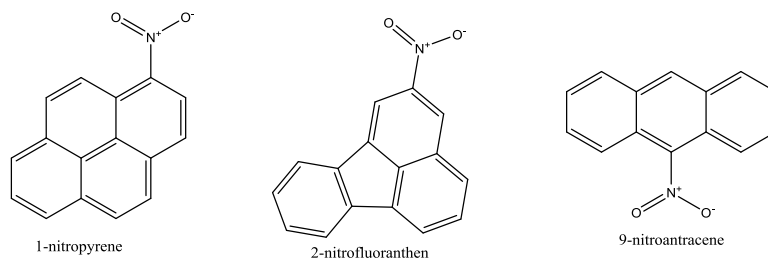


Figure 1.4: Nitrated polycyclic aromatic hydrocarbons that form on particulate matter

The extremely slow reactive nature of NO_2 in the gas phase and fast reactivity at solid surfaces (and in aqueous solution) is likely due to the dimerization of NO_2 to form N_2O_4 that is different in solid (and aqueous) phase from the gas phase (Vione et al., 2006). This example is particularly important as the resultant compounds from the reactivity at the solid-gas (and aqueous) phases are powerful mutagens and suspected

carcinogens. This would help explain the formation of toxic chemical species that are not likely to form under gas phase processing.

Through the examples of the ozone layer, nitrates, and potassium iodide the importance of heterogeneous chemistry is demonstrated and proves that chemistry at solid-gas interfaces are drastically different than that of gas-phase chemical systems. This difference demonstrates that heterogeneous chemistry can be used to better model the chemistry of the atmosphere as these processes occur by different mechanisms and rates when compared to gas-phase chemistry. In addition, molecules can participate in chemistry that is induced by light or- photochemistry. Photochemistry is another important aspect to this study that is discussed below.

1.3 Photochemistry in the Atmosphere

Photochemistry is the study of the chemical reactions that are driven or initiated by light. The sun is the source of light which provides solar radiation that drives photochemical reactions in the atmosphere. The types radiation emitted from the sun include: ultraviolet (100-400 nm), visible (400-700 nm), and near-infrared (700-2500 nm); UV can break chemical bonds, visible excites electrons, and infrared increases the vibrations of chemical bonds. Absorption of light may alter their chemical reactivity of molecules. For example, if UV radiation is absorbed by a molecule, it may dissociate; if a molecule absorbs visible light, the electrons will be promoted to a higher energy level; which may enhance its reactivity. These photochemical changes play an important role in the chemistry of the atmosphere.

There are two major types of processes that can occur upon the absorption of light or solar radiation by atmospheric species: photochemical or photophysical processes. In a photophysical process a molecule absorbs light (this is the equivalent of absorbing a photon), becomes excited and then emits light to reach a ground state via radiative processes such as phosphorescence (emission of light due to a transition between states of different spin multiplicities; theoretically not permitted transitions therefore they have long lifetimes) or fluorescence (emission of light due to transition between states with like multiplicity). The intramolecular transition from one state to another of different multiplicity without the emission of radiation is called intersystem crossing (ISC). The intramolecular transition from one state to another of same multiplicity without the emission of radiation is called internal conversion. Non-radiative photophysical processes may also take place in which the absorbed photons are reemitted as heat (Finalyson-Pitts and Pitts, 2000).

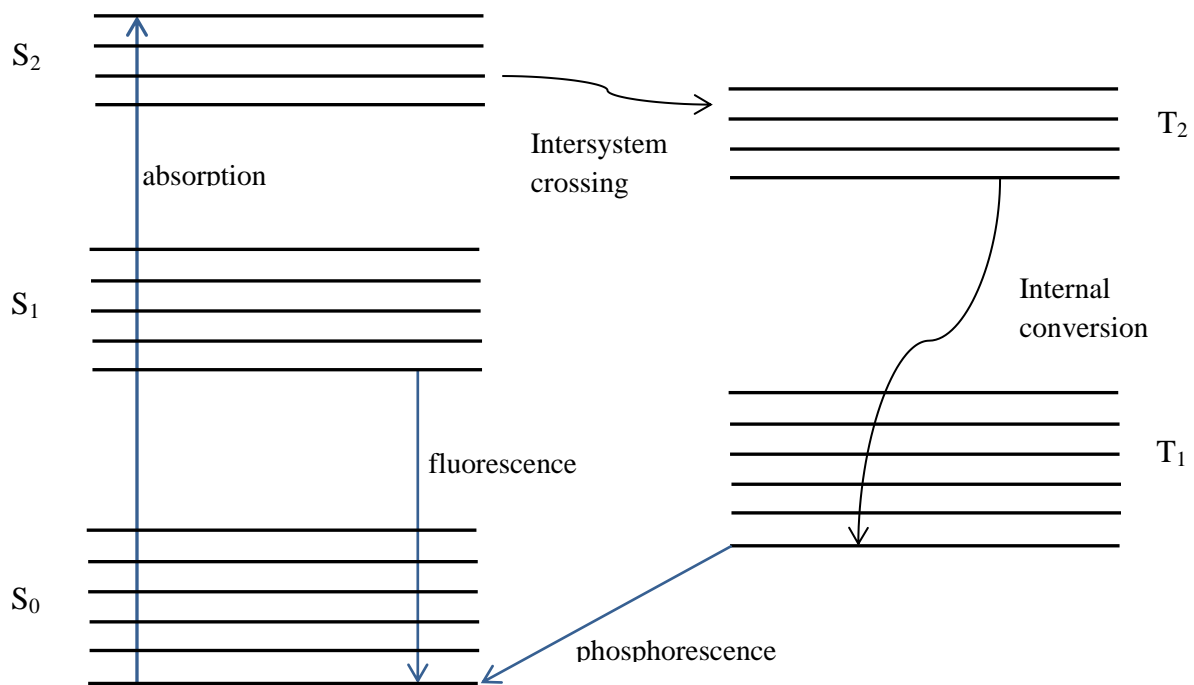


Figure 1.5: schematic of photophysical process

Photochemical processes also involve the absorption of light which induces a chemical change. These chemical changes can involve processes such as photodissociation, intramolecular rearrangements, photoisomerizations, photodimerization, hydrogen atom abstraction, and photosensitized reactions. In the atmosphere several specific reactions occur include: oligomerization, ageing of aerosols, reactivity of semivolatiles, reaction on ocean atmosphere interface, and HONO (nitrous acid) formation. Photosensitized reactions are significant in the atmosphere because the process involves the excitation or reaction of a molecule that would not usually react in the absence of light.

The type of photochemical reaction important to this study is the photosensitization process. This process requires the presence of a light absorbing molecule (the photosensitizer) which induces change in a non-absorbing substrate molecule. Essentially, a photosensitizer absorbs light and transfers the excess energy to another molecule. The chemistry of the molecule that does not readily absorb light may be significantly influenced. A chromophore (light absorbing molecule) absorbs solar radiation which promotes the electrons from a ground state to an excited state. Then, a spin conversion by intersystem crossing occurs from a singlet to triplet state with a certain quantum yield (ϕ). Primary quantum yield quantifies the efficiency of photochemical processes (and photophysical processes) and is defined as:

$$\Phi = \frac{\# \text{ excited molecules proceeding by process } i}{\text{total}(\text{photons absorbed})} \quad \text{Eq 1.1}$$

The change in spin multiplicity (from singlet to triplet) increases the lifetime of the excited state and increases the probability of interacting with another molecule.

There are two major types of pathways following photosensitization processes. The first type involves the triplet state of a photosensitizer reacting with a substrate (other than O₂, such as a phenolic species) to produce a radical species that is derived from a photo-initiated electron transfer or H-atom abstraction between the photosensitizer and another organic that becomes oxidized (see figure 1.6).

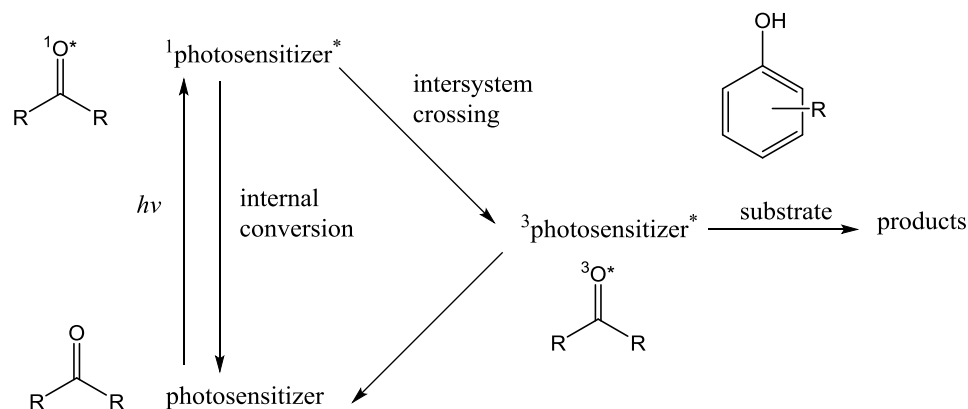


Figure 1.6: A carbonyl photosensitizer is excited to a singlet state, then undergoes intersystem crossing with a specific quantum yield, to produce a photosensitizer that reacts with a substrate, such as a phenolic species. (Adapted from Alvarez et al., 2011)

The other type involves the reaction of the triplet state of the photosensitizer reacts with molecular oxygen (initiated by energy transfer from photosensitizer triplet excited state to O₂). This regenerates the ground state photosensitizer and the formation of singlet state oxygen (see figure 1.7). In this research, we focus on the photochemistry of a photosensitizer with the same compound as the substrate.

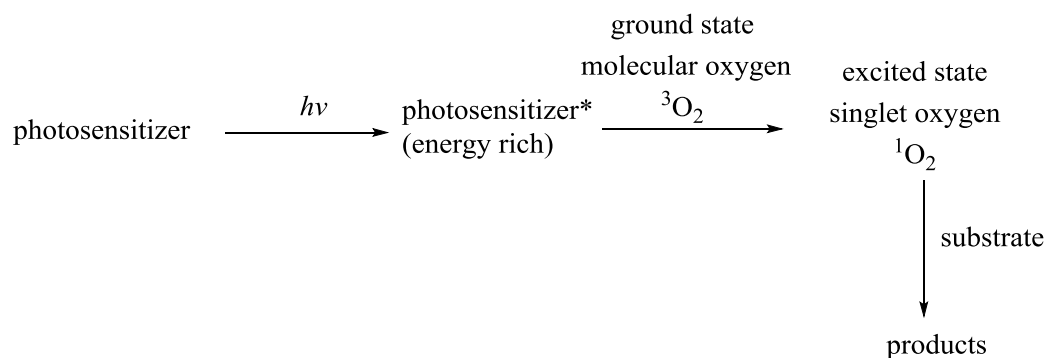


Figure 1.7: Triplet state molecule reaction with excited singlet state molecular oxygen (Adapted from Alvarez et al., 2011).

Sensitized photolysis in aqueous phase organic compounds is known to occur frequently, but much less information exists for aerosol solid phase reactions (Vione et al., 2006). It is possible and likely that the photosensitized reactions that occur in natural water droplets may resemble those in the aerosol solid phase because particulate matter tends to contain photosensitive compounds such as quinones and aromatic carbonyls (some of which are partially derived from polycyclic aromatic hydrocarbons and wood smoke). These compounds on particulate surfaces may also be important sources of OH radicals from the condensed phase; radical formation may be enhanced on aerosol and liquid film surfaces and may generate more photo-oxidation than is known (and used in atmospheric modeling) (Alvarez et al., 2011). Numerous reactions in the atmosphere are driven by the absorption of solar radiation by molecules and interaction with other molecules such as a product of another photochemical process. Other photo-induced reactions may occur by direct photolysis in which the absorption of light breaks a chemical bond and forms reactive radical species (Vione et al., 2006). The troposphere is inherently chemically complex as diverse species react with each other. In the following

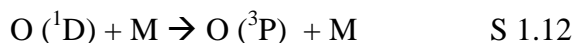
sections important photochemical processes are introduced and described. These photochemical processes are driving forces in tropospheric chemistry.

Formation of tropospheric oxidants via photochemical processes

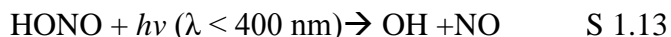
Oxidizing species in the troposphere are highly reactive species that form when precursor species absorb solar radiation. The ageing of many atmospheric species is driven by chemical reactions with these oxidants: hydroxyl radical (OH), atomic chlorine (Cl), nitrate radical (NO₃), hydroperoxyl radical (HO₂), and ozone (O₃). These oxidants are the driving force of a majority of tropospheric chemical reactions and initiate chemical reactions with other reactive species or more stable compounds (which may originate from natural or anthropogenic sources). The formation of the most significant oxidants (OH, NO₃, O₃) and important reactions are described below (Finlayson-Pitts and Pitts, 2000).

Hydroxyl radicals (OH) can come from several sources. OH radicals are products from the ozonolysis of alkenes, free radicals produced by thermal decomposition of peroxyxynitric acid, or dark reactions with NO₃. One major source of OH is the photolysis of ozone (O₃) forming electronically excited O (¹D) (S 1.10). This excited oxygen atom then reacts with water vapor and forms hydroxyl radicals. The majority of excited oxygen atoms, however, are deactivated back to the ground triplet state O (³P) and only a small portion of excited singlet oxygen atoms react to form OH (S 1.12). The OH radical is responsible for the oxidation of many species drives numerous chemical processes important in the atmosphere.

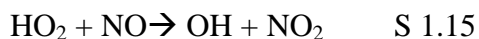




Another source of OH radicals, which is important in polluted areas, is from the photolysis of gaseous nitrous acid (HONO- S 1.13) and hydrogen peroxide (H₂O₂ S 1.14):



In addition when the concentration of NO in the atmosphere is about 10 ppt (parts per trillion), HO₂ sources become sources of OH:



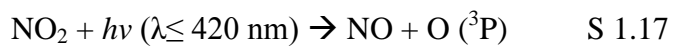
(Finlayson-Pitts and Pitts, 2000).

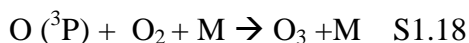
Nitrate radicals (NO₃[•]) are formed by the reaction of ozone and nitrogen dioxide:



(Finlayson-Pitts and Pitts, 2000). Due to its rapid photolysis, nitrate radical chemistry is only significant in the nighttime (strong absorption in the visible region). The photolysis of nitrate radical contributes to the photochemical generation of hydroxyls in the atmospheric waters. It also generates powerful nitrating agents which may cause cancers, developmental effects in humans, and affect cloud and fog composition by the formation of HNO₂ (Vione et al., 2006).

Ozone (O₃) is formed in the lower atmosphere when NO₂ is photolyzed. This leads to a nitric oxide molecule and a triplet state oxygen atom (S 1.17). The triplet state (ground state) oxygen atom then reacts with molecular oxygen to form ozone (Blacet, 1952):





In addition, ozone has a long enough lifetime to continue its chemistry in the nighttime where light is not present.

The chemistry of these photochemically generated oxidants affects the lifetime and fate of many other atmospheric components of various phases. This study focuses on the reactions of one of these oxidants, ozone, with adsorbed organics that participate in heterogeneous and photochemical processes of their own.

1.4 Aerosols, Natural and Anthropogenic, are Ubiquitous in the Atmosphere

Tropospheric aerosols originate from natural and anthropogenic sources; the composition of the aerosol usually indicates the source that is responsible for its release into the atmosphere. The total mass of natural aerosols such as mineral dusts, globally, is considerably higher than that of aerosols that of anthropogenic aerosols such as sulfates, organics and black carbon (Ma et al., 2008).

Several well characterized aerosols include mineral dusts, sea salts, and black carbon. One of the most significant natural aerosols, dust, is introduced into arid and semiarid regions as a result of dust storms. Approximately 1000 to 5000 Tg of dust are introduced into the atmosphere from dust storms and thus has become important factors to consider while studying climatic changes (Xu et al., 2010). Another natural aerosol, sea salt aerosols, from sea spray at the Marine Atmospheric Boundary Layer (MABL), are produced at a rate of 3300 Tg per year and account for 30-75% of the global budget of all natural aerosols (Jacobson, 2001).

Black carbon (BC) is comprised of mostly elemental carbon and originates from incomplete combustion of certain organics from anthropogenic or natural sources, such as burning fossil fuels, biomass combustion and natural forest fires (Winter and Chylek, 1997). Annual emissions of black carbon are 12 Tg which may not seem as a significant amount, but is second only to CO₂ as a climate change contributor (Pennar, 1998). Annual aerosol emissions are shown in Table 1 with the known compounds they are comprised of. The contributions of fossil fuel, biofuel, and open burning are estimated as 38%, 20%, and 42%, respectively for black carbon, and 7%, 19%, and 74%, respectively, for organic carbon (Bond et al., 2004).

Table 1.1. Annual aerosol emissions or abundance; Teragram (Tg)= 10¹² grams (Pennar 1998)

Aerosol	Annual Abundance (Tg /Year)	Main Chemical Compounds
Mineral Dust	1,000-5,000	SiO ₂ , Al ₂ O ₃ , CaCO ₃ , clays
Sea Salt	3,300	NaCl, NaBr, KI
Sulfates	200	
Organics	138	
Nitrates	18	
Black Carbon	12	

1.5 Biomass combustion releases methoxyphenols and other compounds

Biomass combustion, or burning of natural materials, is a major source of fine organic particulate matter (<2.5 μm) that can contribute to a significant portion of the total organic fraction of aerosols in the troposphere (Net et al., 2011). Organic particulate matter that originates from the combustion of biomass such as wood is the core aspect of this research project because of its contribution to organic aerosols.

Wood is a complex material that is composed of lignocelluloses, which include three biological polymers: cellulose, hemicelluloses and lignin (Garcia-Maraver et al.,

2013; Krecl et al., 2007), that account for approximately 40-50%, 18-35%, and 25-35% the mass of dry wood, respectively (Parham and Gray, 1984; Petterson, 1984; Cheremisnoff, 1980). Upon burning, these polymers breakdown into component monomers and are released into the atmosphere as fine particulate matter, volatile organic compounds, or semivolatile organic compounds. The major organic compounds emitted directly into the smoke particles are straight chain aliphatic compounds from vegetation wax and diterpenoid acids from resin (Oros and Simoneit, 2001). Major natural products include monosaccharide biopolymers and phenolic products, which are produced from combustion of cellulose and lignin, respectively (Oros and Simoneit, 2001).

Lignin pyrolysis products (the resulting molecules emitted as a result of the breakdown of wood during a fire, see figure 1.8 for common molecules and structures) are major component in wood smoke (Net et al., 2011). Lignin is comprised of monolignols which can be broken down into the building blocks of the material such as phenols, methoxyphenols (guaiacols), and dimethoxyphenols (syringols).

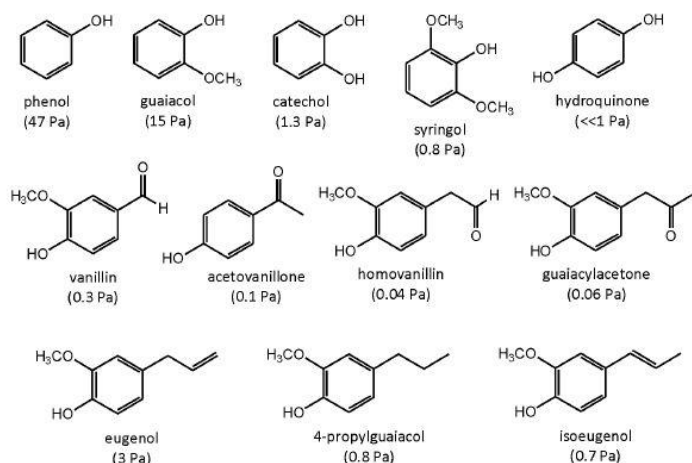


Figure 1.8: Common lignin pyrolysis products with vapor pressures listed below structure in Pa. (Adapted from O'Neill et al., 2013)

Many methoxyphenols are semi-volatile organic compounds (SVOCs); they have vapor pressures high enough to allow them to subsist as gases in the atmosphere and simultaneously low enough to adsorb onto other aerosol surfaces. Several known lignin pyrolysis products with relevant vapor pressures are shown in figure 1.8. This allows biomass burning aerosols to be comprised of mixtures of numerous compounds on a single substrate. Several lignin pyrolysis products have been shown to adsorb on other aerosols such as minerals dusts (SiO_2 , Al_2O_3) and sea salt aerosols (NaCl) in laboratory models designed to determine their chemical behavior (Net, 2011; O'Neill et al., 2013).

Other species are emitted in forest fire smoke that can be used as tracers (compounds that indicate emission from wood smoke). Biomass burning aerosols are usually composed of organic carbon (such as mixtures of methoxyphenols - lignin pyrolysis products) and inorganics such as potassium chloride. The aerosols emitted in biomass burning show a unique characteristic high concentration of organic carbon compound as well as water soluble potassium. The concentrations of these components are > 10% for organic carbon compounds and approximately 1-10% water soluble potassium (Duan, 2003). Due to its high concentration in these aerosols, potassium is the most common biomass burning aerosol and is the most commonly used tracer (Simoneit, 2000). Thus, potassium containing aerosols such as potassium chloride (KCl) is a good model for solid phase surface on which biomass organics can adsorb.

Methoxyphenols and potassium chloride are used as tracers for wood smoke, although their reactivity in the atmosphere has not been well characterized (Simoneit and Elias, 2001; Simoneit, 1999; Simoneit, 2002; Hawthorne et al., 1898). The lack of understanding of the reactivity of these types of compounds is the motivation behind this

research project. Understanding the chemistry of these compounds will help determine the chemical properties and evolution of these compounds as they mix and travel through the atmosphere. Due to the pervasiveness of these compounds much can be determined about their chemical behavior is appropriate models are selected.

1.6 Chemical Diversity is Common on Single Substrates

Aerosols are constantly moving around Earth's atmosphere and mix together to form aerosols with different chemical properties. NASA has generated a high resolution model with its Discover supercomputer to illustrate the displacement and mixing of aerosols. A still image of the prediction is shown in figure 1.9.

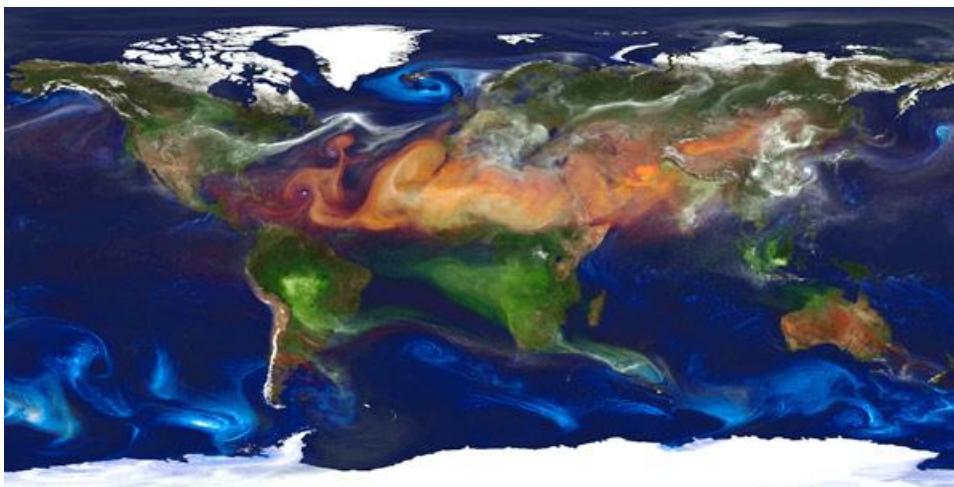


Figure 1.9: Image still from NASA Discover supercomputer generated video displays aerosols moving across the Earth's surface and show mixing of aerosols. Dust (Red), sulfate (white), organic and black carbon (green) and sea salt (blue) are shown. Full video can be found at <http://www.youtube.com/watch?v=zgFSpHL2k8I>

Although it may seem aerosols exist in a state of chemical uniformity, this is not the case. In aircraft field studies over Mexico City, samples collected on a single carbon filter have shown numerous elemental and compound components mixed together,

including organic matter traced to vehicle exhaust and biomass combustion. Other elements such as sodium, potassium and aluminum were also identified (Adachi and Buseck, 2008). The mixing, a more accurate image of aerosols, has severely complicated attempts to accurately study aerosol's chemical behavior and evolution. In addition, mineral dusts mostly comprised of SiO_2 and Al_2O_3 have high surface areas that provide reactive sites that can alter the composition and toxicity of aerosols, affect the composition of the atmosphere through the adsorption of gases, and are known to take up organic compounds (Buseck, 1996). Oxidation at these surfaces is known to occur under irradiation and in dark conditions (Raff et al., 2010). Other atmospheric components like ammonium sulfate can be coated with organics such as palmitic acid and can act as ice nucleation sites (Wise, 2010).

Aerosols act as substrates for different chemical compounds and provide a surface for reactivity. These reactions can alter natural cycles and behaviors of the atmospheric components. Aerosols complex composition and chemistry may play a significant role in the dynamics of climate change.

1.7 Aerosol's role in climate change is associated with uncertainty

Climate change is one the most significant environmental issues that has been comprehensively studied. The increase in global temperatures is attributed to the expansion of human activity to the Greenhouse Effect. As solar radiation reaches the Earth's surface and warms it, a significant amount of solar radiation is reflected back out to space. Greenhouse gases such as water vapor, carbon dioxide, methane and nitrous oxide absorb infrared radiation that is emitted by the Earth. The parameter used to

quantify the difference in solar radiation reaching the surface of the Earth and remission is called Radiative Forcing (RF); positive values like the ones that are characteristic of greenhouse gases point to warming effects, while negative values indicate cooling effects. The Greenhouse effect may be the major cause of climate change, but another component in the atmosphere may be significantly affecting the climate, namely aerosols.

There are two major types of climatic effects that aerosols have: direct effects and indirect effects. The direct effect of aerosol's can be subdivided into two types. The first type involves aerosol's ability to absorb incoming solar radiation and reemit it as heat producing a net heating effect on the Earth's surface. The second involves the aerosol reflecting incoming solar radiation and producing a net cooling effect. The indirect effect of aerosols is based on the idea of aerosol's ability to act as cloud condensation nuclei. Water vapor requires a surface to condense onto to form clouds; aerosols provide numerous surfaces and create white clouds that reflect incoming solar radiation and result in net cooling on the Earth's surface. An illustration of these effects is shown in figure 1.10 and illustrates the relationship of solar radiation and aerosols to climate.

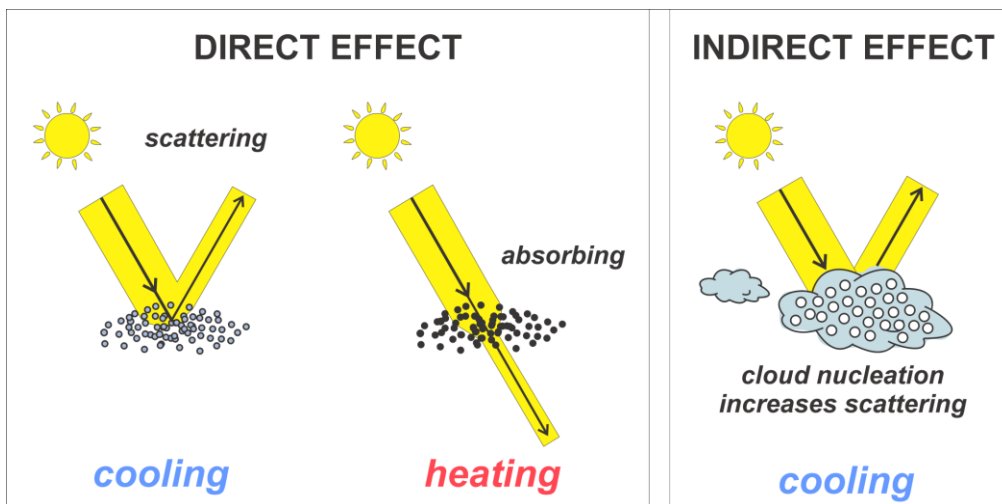


Figure 1.10: Direct and indirect effect of aerosols; aerosols can provide net cooling or net heating effects depending on the composition and type of effect of the aerosol (Adapted from R.Z.Hinrichs, 2012).

The various climatic effects of aerosols depend on their chemical composition and reactivity. Since aerosols are extremely chemically diverse and can undergo many chemical reactions that change their composition, the climatic impacts of aerosols are uncertain. According to the recent report from the Intergovernmental Panel on Climate Change (IPCC), the radiative forcing of aerosols contributes to the largest uncertainty in the total radiative forcing estimate (IPCC, 2013). The uncertainty in RF associated with aerosols is shown in Figure 1.11 under the “Aerosols and precursors” portion of the table and shows that the uncertainty, shown with an error bar, stretches from positive to negative RF values.

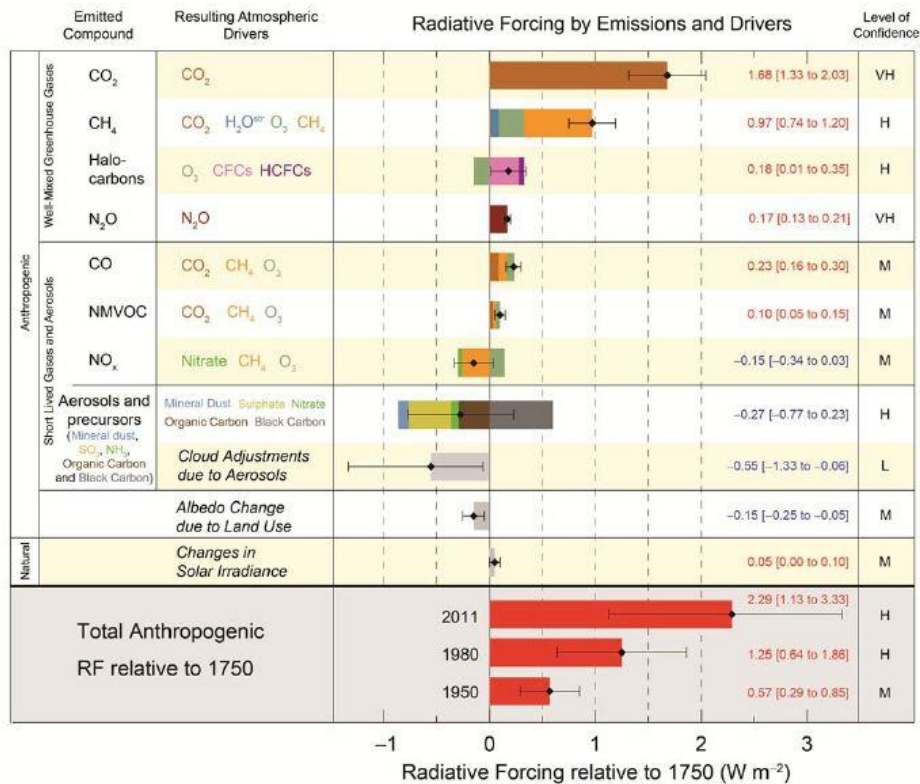


Figure 1.11: total radiative forcing according to the IPCC 2013 report shows the large error bar indicating the uncertainty associated with the climatic effects of aerosols.

The uncertainty in the estimated RF can be decreased if appropriate models are designed to imitate these aerosols' chemical behavior in the atmosphere and provide quantitative and insightful results to be used in computational modeling.

1.8 Modeling adsorbed lignin pyrolysis product reactions requires atmospheric relevance

To model the processes that lignin pyrolysis products undergo in the troposphere and obtain quantifiable kinetic information, simplifying the system is necessary. Each atmospheric aspect must be tested to reveal its significance. There are many factors in the atmosphere that can affect aerosols' chemistry such as oxidation by various atmospheric pollutants, solar radiation exposure and humidity effects. Previously discussed factors such as heterogeneous chemistry and photochemistry must be included in models to obtain applicable atmospheric models. The model system of choice involves a solid phase aerosol substrate, semi-volatile lignin pyrolysis product, a tropospheric pollutant, and simulated solar irradiance. This will guide the experimental setup.

Ozone which results in one source of oxidation of methoxyphenols can produce secondary organic aerosols (Net et al., 2011) which may alter their vapor pressures and affect aerosol composition, reactivity, and absorption properties. The reactions of adsorbed organics with ozone are also of particular interest because of the well-known reactivity ozone displays. Since it exists in the troposphere as a pollutant and is highly reactive, it will likely contribute to the heterogeneous chemistry of the troposphere. A great deal is known about gas phase oxidation by ozone (O_3), but very little is known

about the oxidation of organics adsorbed on surfaces (Karagulian et al., 2008). Another important factor to consider is the effect of solar radiation on aerosol chemistry. Certain lignin pyrolysis products are phenolic or carbonyl containing species that are known to exhibit photo-sensitized processes but the exact mechanisms, effects, and rates are unknown (Alvarez et al., 2011). Because photochemistry is known to have major influences on atmospheric species, as discussed earlier, this aspect is crucial to understanding aerosol chemistry.

In understanding the qualities lignin pyrolysis products possess such as adsorption properties, ability to engage in heterogeneous chemistry with gaseous species such as ozone, and effects of solar irradiation, a laboratory aerosol model can be designed to understand the combination of these effects. These heterogeneous systems have been recognized as species with significantly different properties than their components and thus studying them will provide a more accurate image of the chemistry of aerosols to clear out the uncertainty in the climatic impacts associated with them. Designing experiments that show how long these aerosols persist in the atmosphere, or obtaining kinetic information, will elucidate their real behavior in the atmosphere and allow for the design of models that accurately depict climate change patterns and the chemistry of the troposphere.

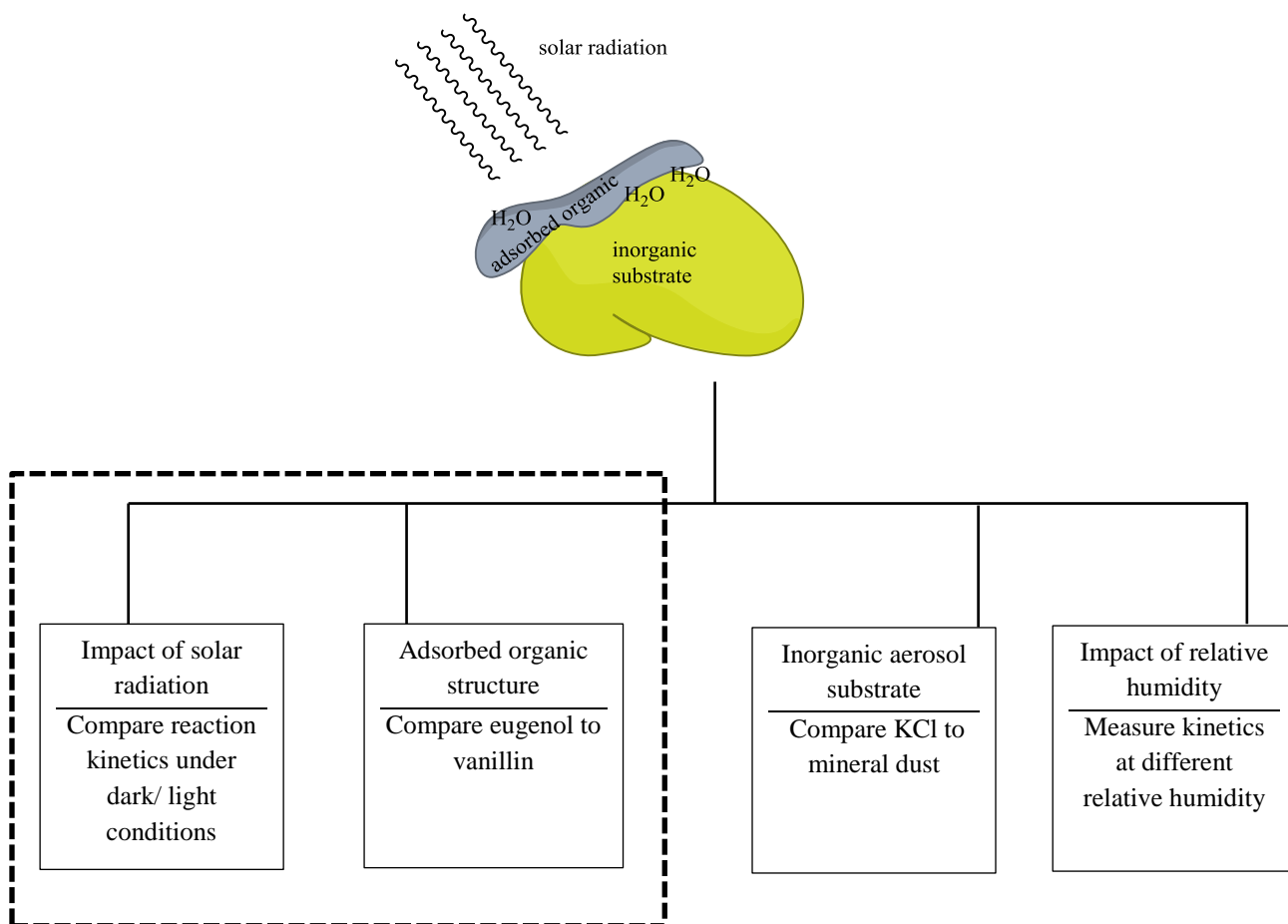


Figure 1.12: Schematic showing the factors that affect the chemistry of tropospheric aerosols. The factors enclosed in the dashed box are considered in this thesis.

1.9 Designing a representative atmospheric model to obtain quantitative information

To build a conceptual framework for understanding the reactivity of lignin pyrolysis products, we selected representative compounds to investigate the

photochemistry of broad classes of adsorbed tropospheric organics. Common lignin pyrolysis products are listed in Table 1.2.

Table 1.2: common lignin pyrolysis products of interest and total emission factors (quantity of species released into the atmosphere)

Lignin pyrolysis product	Total emission factor (mg/kg)
Vanillin	57
Vanillic acid	168
Acetovanillone	166
Homovanillyl alcohol	101
Acetosyringone	31
Syringaldehyde	182
Catechol	177
Eugenol	17

Two model lignin pyrolysis products have been chosen for this study: vanillin and eugenol. Eugenol is a common lignin pyrolysis product with a vapor pressure of 0.6 kPa and has an emission factor of 17034 $\mu\text{g}/\text{kg}$ from conifer smoke (Oros and Simoneit, 2001). The eugenol side chain consists of a terminal double bond (see figure 1.13 for structure).

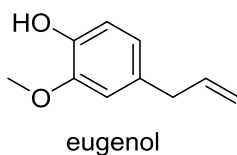


Figure 1.13: structure of eugenol, the lignin pyrolysis product that will be used to coat the inorganic substrate in this study.

Previous literature shows that upon exposure to ozone, adsorbed eugenol undergoes oxidation when adsorbed onto alumina and sodium chloride (O'Neill et al., 2013). Side chain oxidation occurs, as well as ring cleavage which provides a potential for photo-enhancement of oxidation. The ring cleavage products and oxidized side chains

could potentially become photosensitizers. Many other types of lignin pyrolysis products with similar structures may display similar behavior and this study will allow for the prediction of their behavior in the troposphere.

The other model lignin pyrolysis product of choice for these studies is vanillin which has an emission rate of 15mg/kg, total emission factor of 57 mg/kg from conifer smoke and vapor pressure of 0.3 Pa (Oros and Simoneit, 2001; Net et al., 2011). This major molecular tracer has a vapor pressure that is on the same order of magnitude of eugenol derivatives such as isoeugenol and 4-propylguaiacol which have shown reactivity while adsorbed onto sea salt (O'Neill et al., 2013). Previous studies on silica particles with adsorbed vanillin detect vanillic acid but do not detect ring cleaved products as with eugenol (Net et al., 2011). It is likely that the difference adsorption onto sea salt aerosols and mineral dust play a major role in reactivity, so it is necessary to study binding mechanisms with inorganic aerosols. Vanillin is also of particular interest because of its potential ability to act as a photosensitizer; it contains an aromatic and phenolic carbonyl (see figure 1.14).

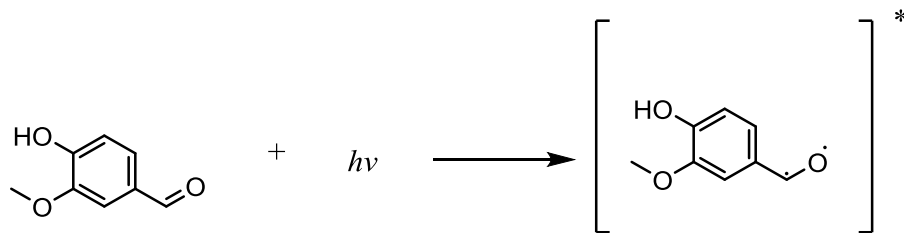


Figure 1.14: triplet state of vanillin after photo-sensitization demonstrates varying reactivity compared to other methoxyphenols.

Vanillin contains both species (phenol and carbonyl) observed in this type of mechanism and it is likely to undergo this process with itself in the presence of light.

The chemistry of the model lignin pyrolysis products vanillin and eugenol will be studied by adsorbing them onto a potassium chloride substrate and quantifying the kinetic parameters associated with the reactions in the presence of ozone and light. By studying the kinetics of the photo-reactions of eugenol and vanillin we can gain a clearer understanding of the fate of these organics and their lifetimes in the atmosphere to clear up the uncertainty associated with their chemical properties and climatic impacts. These kinetic parameters will be beneficial in atmospheric computational modeling to predict chemical ageing of these species.

Chapter 2: Experimental Methods and Techniques

The experimental techniques and underlying theories are discussed in this chapter. The focus here is on the data obtained from the techniques and the interpretation and analysis of the quantitative data. The techniques described below are important for revealing kinetic parameters (chemical reaction speed) and supporting information to describe the photochemistry of the ozonolysis of adsorbed eugenol and vanillin.

To understand the impact of the ozonolysis of eugenol and vanillin in the presence and absence of light, the products of the reaction were identified. The identification of the products will illuminate the ageing that these model compounds undergo in the atmosphere and understand their influences on the troposphere. Two major techniques were used to identify the products which are ^1H NMR and GC-MS. In the following section the underlying theory of these techniques is explained in addition to the experimental techniques used to obtain the identities of the product compounds. First, kinetic techniques are described followed by product identification techniques.

2.1 Why Study Reaction Kinetics?

Numerous complicated chemical reactions occur throughout the atmosphere on aerosol surfaces, therefore undertaking experiments to understand all chemical reactions is a challenge. The number of reactions that ought to be studied can be narrowed down by quantifying the rates of different chemical reaction. Chemical reactions that occur very slowly may be insignificant because the species remain unchanged for a long period of time, which means their atmospheric influences may be minimal. Reactions that occur very quickly are influencing the atmosphere's chemistry thus they become significant. This is particularly important with adsorbed organic compounds on aerosols which

undergo numerous chemical reactions with ozone (O₃). Kinetic information obtained will be used to calculate atmospheric lifetimes and can be used in computational modeling used to predict climate change.

2.2 What are Reaction Kinetics?

The kinetics of a chemical reaction quantifies the rate of the reaction or the change of concentrations of reactants over a time interval. The rate of the reaction can be calculated from the concentrations of the reactants and the rate constant k -an experimentally determined value specific to each chemical reaction. For a generic elementary chemical reaction (single transition state),



the rate law can be written as follows:

$$\text{Rate} = -\frac{1}{a} \frac{d[A]}{dt} = k[A]^a[B]^b \quad \text{S 2.2}$$

Where a and b are the stoichiometric coefficients, k is the proportionality or rate constant, and $[A]$ and $[B]$ are the concentrations of the reactants. The stoichiometric coefficients are not always equal to the exponents in the rate law; this is the case for non-elementary reactions in which case exponents need to be determined experimentally by holding reactant concentrations constant.

2.3 How Was Kinetic Data Obtained?

Kinetic information was collected via a specific type of Infrared Spectroscopy (IR), a commonly used analytical technique that is best suited for these experiments. This

technique is called *Diffuse reflectance infrared Fourier transform spectroscopy* or DRIFTS. DRIFTS allowed us to monitor the adsorption of gas phase methoxyphenol onto the solid surface. Subsequent reactions with ozone in the presence and absence of light were also monitored over time with DRIFTS.

2.3 Infrared Spectroscopy, a look into the underlying theory

The heterogeneous chemistry of surface adsorbed vanillin and eugenol on KCl was studied by using infrared spectroscopy. Infrared spectroscopy is an analytical technique commonly used to identify functional groups in molecules by using infrared radiation (IR) to excite molecules to higher vibrational modes. The bonds that hold molecules together are dynamic and can be modeled as springs holding two atoms together. Since these springs, or bonds, are constantly vibrating with a specific frequency, they can absorb different wavelengths of energy that can excite their vibrations to higher frequencies which can be predicted by equation 2.1.

$$\nu = \frac{1}{2\pi} \sqrt{\frac{k}{\mu}} \quad \text{Eq. 2.1}$$

The frequency (cm^{-1}) of the bond is described by equation 2.1 in which the k is proportional to the strength of the bond (spring constant) and μ is the reduced mass between two atoms described by equation 2.

$$\mu = \frac{m_1 m_2}{m_1 + m_2} \quad \text{Eq. 2.2}$$

The reduced mass is equal to the product of the two masses of the atoms divided by the sum of the two masses. The frequencies that bonds can vibrate at are specific for certain

types of bonds between specific atoms. This allows us to monitor specific bonds, which are known to absorb and vibrate at certain frequencies.

The model that describes the excitation of molecular vibrations is based on a quantum mechanical model. The quantization or discrete property, of the energy levels of vibrational modes of the bonds is described in a potential energy well, where energy levels are equally spaced. The “energy well” shown in Figure 2.1 is based on the harmonic oscillator model shown in equation 2.3 that describes the relationship of the attractive force k that holds the bonds together and the distance that separates them x . The distance between the bottom of the well and lowest vibrational state is called the “zero-point energy” because the molecule still exhibits vibrational energy at the ground state. The energy transition that occurs with the absorption of a photon, in this case a photon with IR wavelength, excites the molecule to the higher vibrational mode. A potential energy well is shown in figure 2.1 and illustrates the relationship between energy and the distance between the two atoms.

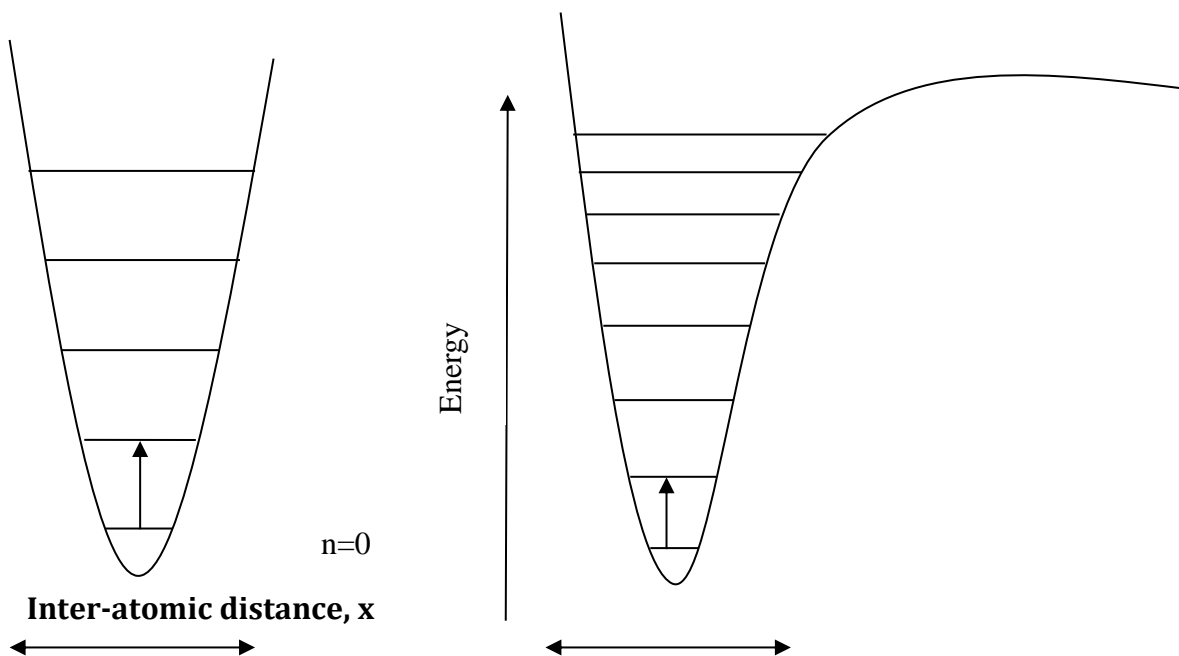


Figure 2.1 Potential energy diagrams (energy wells) (left) harmonic oscillator model excluding nuclear repulsion, (right) anharmonic oscillator, $n=0$ is lowest energy point in well, or zero point energy. Arrows from ground state indicate absorption of IR photon and excitation to higher vibrational mode or energy.

The atoms are modeled as masses on a spring like a harmonic oscillator, however the repulsive forces that occur between two atoms is excluded. The energy well in figure 2.1 shows the repulsive forces that occur when the distance between the two atoms becomes too small, repel and then dissociate resulting in the anharmonic oscillator.

$$E = \frac{1}{2}kx^2 \quad \text{Eq. 2.3}$$

$$E = h\nu\left(n + \frac{1}{2}\right) \quad \text{Eq. 2.4}$$

The absorbance of a photon is quantified by equation 2.6, where the absorbance is equal to the negative logarithmic ratio of the transmitted radiation (I) to the incident radiation (I_0).

$$Absorbance = -\log\left(\frac{I}{I_0}\right) \quad \text{Eq. 2.6}$$

As a molecule absorbs incoming IR radiation the molecule vibrates at a higher frequency equal to the energy of the absorbed photon. This is illustrated in figure 2.1, as excited states in the energy wells, or potential energy diagrams.

As mentioned above the specific type of IR called DRIFTS was used in these experiments. DRIFTS is different from commonly used IR spectroscopy because the measured or detected signal is a *diffused and reflected beam as opposed to a direct transmittance or absorbance*. When a focused beam reflects off fine crystals it is scattered in all directions and the IR that is detected is a reflected and scattered beam. The scattered beam is re-focused onto a mirror and directed to a detector. DRIFTS is most useful for powdered solid samples such as the fine and high surface area KCl crystals used in this experiment because the IR beam makes direct contact with the solid. In addition, KCl does not absorb in the infrared region of the electromagnetic spectrum, thus only the reactions with the methoxyphenol (which strongly absorb in the IR region) are monitored without interference from the KCl crystals. DRIFTS allows us to study the surfaces coated with the methoxyphenol which is the essence of the heterogeneous chemistry.

2.5 Experimental Setup

Diffuse reflectance infrared Fourier transform spectroscopy was used to monitor the ozonolysis of adsorbed organic (eugenol and vanillin) on a potassium chloride surrogate in the presence and absence of light. Pure KCl crystals (Sigma Aldrich, >99.0% purity) were ground into a fine powder via mechanical ball mill (Wig-L-Bug) for 5 minutes. Fine powdered KCl, 100 mg, was packed into DRIFTS chamber and heated to 300°C for 1 hour under constant air flow (760 sccm, zero grade) until RH was <2% . Potassium chloride sample (Sigma Aldrich 99% purity) was allowed to cool to room temperature under constant air flow. A background spectrum of uncoated KCl was collected; KCl was then coated with organic. Adsorption or coating was achieved by passing constant air supply through bubbler containing organic to volatilize into gas phase (room temperature phase: liquid eugenol, solid vanillin). Gas phase organic absorbed onto KCl while running through DRIFTS chamber until saturation. A 45 minute purge followed organic coating until to remove excess organic in tubing and prevent desorption during ozonolysis. Adsorption was monitored by collecting a spectrum every 1.05 minutes (64 scans, resolution: 4 interferogram: max amplitude 6.5) by a Nicolet 6700 FT-IR with a photoconductive MCT detector (HgCdTe).

The reaction with ozone was monitored in the exact manner the adsorption was monitored. The DRIFTS chamber used ZnSe windows which are compatible with ozone. A schematic of the experimental setup is shown in Figure 2.2.

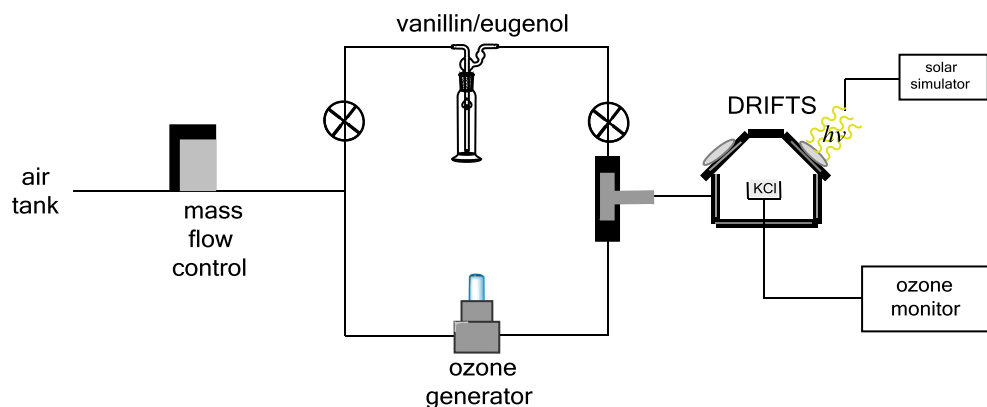


Figure 2.2: experimental schematic for reactions of adsorbed organic (vanillin or eugenol) onto KCl substrate with ozone under simulated light

Ozone was generated by a Jelight Double Bore® lamp and monitored by a Jelight 465L ozone monitor. Ozone concentrations measured were between 150 ppb-6 ppm. Light reactions used a Newport solar simulator light source (xenon lamp) that was turned on and off at certain (10-15 minute) intervals in specific experiments. The solar simulator was turned on or off throughout course of some experiments to obtain kinetic data for light or dark conditions experiment. A water filter was used to keep temperature constant and remove IR so sample does not heat up. The solar irradiance range from 300-700 nm was accomplished by blocking majority of UV light with a glass filter as shown in Figure 2.3. Experiments were conducted over the course of 800 minutes under steady laboratory conditions.

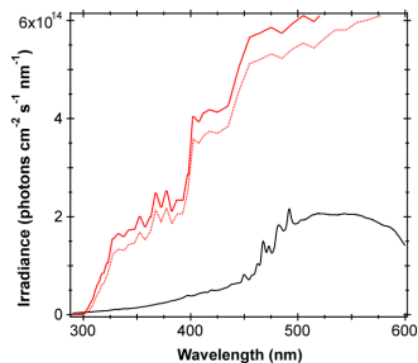


Figure 2.3: solar simulator irradiance with glass filter in black. Red lines show the actinic flux at 0 (solid) and 40 (dotted) zenith angles; this shows irradiance reaching Earth's surface. (Adapted from R.Z. Hinrichs .)

2.6 An Introduction to NMR

NMR was used to identify the products from the reactions of KCl adsorbed organic. Nuclear Magnetic Resonance (NMR) exploits a nucleus's spin in a magnetic field to ultimately identify the structure of a molecule. Nuclei rotate around an axis, a trait called spin, with a specific angular momentum that is quantized. The maximum number of components of the angular momentum of the nucleus's spin is $2I + 1$, where I is the spin quantum number. In the absence of an external magnetic field, the different states have equal energies. Four nuclei are the most commonly used in chemical analysis which include, ^1H , ^{13}C , ^{19}F , ^{31}P . The specific type of NMR used to identify products in this study is proton NMR (^1H NMR), which is based on the magnetic moment around protons.

When a charged nucleus "spins", it creates a magnetic field that is similar to the magnetic field produced around electricity flowing through a coiled wire. The resulting magnetic moment is oriented along the axis of the spin and is proportional to the angular

momentum. The proportionality constant is the magnetogyric ratio (γ) which is a specific value for each nucleus (it also is proportionality constant for the frequency of absorbed energy and the magnetic field strength) (Skoog et al., 2007).

The nucleus that spins has a magnetic moment proportional to the spin. When an external magnetic field is applied B_o , two spin states ($m = +1/2$ and $-1/2$) occur, one is aligned with the field ($+1/2$, lower energy) and the other against the field ($-1/2$, higher energy). The energy difference between the spin states (measured in MHz) depends on the applied external magnetic field and the nucleus being studied. Irradiating the sample with radio frequency energy that corresponds to the spin state separation will cause $+1/2$ to go to the higher $-1/2$ state. The energy difference will be proportional to the magnetic moments (Skoog et al., 2007). Thus the energy of the states is equal to:

$$E = \frac{-\gamma m h}{2\pi} \quad \text{Eq. 5.1}$$

Where m is the spin state and h is Planck's constant. Radio frequency applied to the field is required to bring a change in the alignment of the magnetic moment of the proton from a direction where it is parallel to the field to one where it is anti-parallel (Skoog et al., 2007).

To obtain data from the NMR, the nuclei in the strong magnetic field are exposed to extremely fast and brief radio frequency pulses usually under $10 \mu\text{s}$, with the frequency at 10^2 to 10^3 MHz (mega Hertz). The interval between each pulse lasts for a few seconds, during which a time domain RF signal (called the FID or free induction decay) is emitted as the nuclei relax and is detected by a receiver coil (the same coil

sends the radiofrequency pulses). The time domain data are added up and converted to a frequency domain signal (Skoog et al., 2007). The time to frequency domain conversion is a Fourier transform which allows the output data to be interpreted as chemical shifts based on the electronic environment around the nuclei. Electronic shielding which occurs when there is a high density of electrons around a proton which results in a high field signal; desheilding occurs when the atom is exposed to a decreased electronic density and shows a low-field signal.

2.7 Experimental Techniques for NMR

The reaction of the adsorbed methoxyphenol on a NaCl substrate (similar chemical properties to KCl) in ozone was conducted by placing 1g of substrate onto a fritted disk (gas permeable) in a glass stem and connecting airflows directly to the stem. The methoxyphenol adsorption process was conducted in a similar manner to the kinetic studies' in which air flow carried gas-phase organic onto the substrate, although the adsorption time was significantly longer (approximately 16 hours). Reaction with ozone followed and lasted for approximately 120 hours. For light reactions the solar simulator irradiated directly onto the sample, which was shielded from external light sources.

After the reaction was completed, the substrate with adsorbed products were removed from the apparatus and placed in an 8-dram vial with approximately 4 mL deuterated acetone (Aldrich, 99% 0.03% TMS). The mixture was sonicated (exposure to ultrasound waves) for ~1 hour and substrate was allowed to settle. Solution of products and deuterated acetone were transferred (~0.7 mL of solution) without filtration into

NMR tube for analysis. NMR analysis was conducted with a 200 MHz Bruker NMR (approximately 30,000 scans).

2.8 An Introduction to GC-MS

GC-MS, Gas chromatography mass spectrometry are two distinct techniques combined into one instrument. Gas chromatography is a separation technique; mass spectrometry is the detector in this instrument that analyzes mass fragments to help determine the structure of compounds.

Gas chromatography uses a carrier gas to transport a gaseous sample through a column. The sample is injected into a heated septum and then quickly evaporates. The sample travels through the column (fused silica) with the carrier gas (an inert gas such as He or N₂) separating the components in the sample based on retention times that depend on the compounds volatility. A compound with high volatility will have a low retention time; a compound with low volatility will have a high retention time and elute out last.

The compounds then reach the end of the column to the detector, in this case a mass spectrometer. The mass spectrometer produces an ion source where the molecules are ionized by the bombardment of free electrons (produced by a filament). Many ionized molecules fragment into characteristic fragmentation patterns. Collisions that ionize the molecule may not fragment the molecule, but produce the cation. These species are then accelerated by an electric field to a mass analyzer. In most instruments the electric field produced directs the fragments to different parts of the detector depending on their mass. The location of the fragments “landing” on the detector is used to determine their mass or molecular weight based on the probabilities. These fragments are identified by the NIST

library which contains numerous fragmentation patterns used to identify the fragments and parent molecules.

2.9 GC-MS Specifications and Techniques

Samples obtained from DRIFTS experiments were analyzed using GC-MS. DRIFTS samples were sonicated in acetonitrile (similar to above), transferred to amber vials and filtered through a 0.2 μm syringe filter. Samples were derivitized by adding approximately 8 drops (1 drop is about 0.010 mL) of N,O-Bis(trimethylsilyl)-trifluoroacetamide (BSTFA). This compound reduces the polarity and enhances thermal stability by adding trimethylsilyl (TMS) groups to susceptible functional groups by replacing H on hydroxyl groups and carboxylic acid groups. The column used was a Supelco SLB-5ms, 30m x 0.25 mm x 0.25 μm film thickness column. 1.0 μL , Pulsed Splitless injections were used due to low concentrations. All analysis was conducted with an Agilent Technologies GC-MS (6890N-GC/5973-MS) with a Supelco SLB-5ms column with oven temperature cycles of 100°C for 2 minutes then 12°C per minute to 200°C for 5 minutes with a total run time of 15 minutes. (Van Ry, 2013; Van Ry, 2012).

Chapter 3: Results and Discussion: Vanillin

To understand and quantify the effects of simulated solar radiation on the ozonolysis of KCl adsorbed vanillin, data collected from experiments conducted in the dark were compared to experiments under light conditions. The analysis of collected data involved several aspects: first, important functional groups were identified in IR spectra which helped determine the products of the reaction. Second, GC-MS was used to further identify the reaction products. Third, specific functional groups were integrated over time to measure a rate of loss or growth; this allowed kinetic parameters were obtained by fitting exponential functions to the integrated kinetic curves, and the resulting experimental rate constants were analyzed as a function of ozone concentration.. The significance of these reactions was determined by quantifying the kinetics of these reactions. Identification of functional groups from IR spectra was also used to predict the products of these reactions and was supported with GC-MS analysis. The details of analysis are further integrated into the discussion below.

3.1 Identification of Functional Groups in IR Spectra

Central to this study is the heterogeneous chemistry associated with adsorbed methoxyphenols. Thus, it is extremely important to prove that gaseous vanillin does indeed adsorb onto the KCl substrate. A recorded DRIFTS spectrum of adsorbate onto the KCl substrate shows that the adsorption of an organic onto the surface does occur; DRIFTS only records the molecular vibrations on the solid surface and not in the gas phase, thus any molecular vibrations observed occur on the surface. It must also be confirmed that the vibrations shown at the surface, as seen in Figure 3.1 correspond to

vanillin molecular vibrations. A list of identified functional groups is shown in Table 3.1 and the structure of vanillin is shown for reference.

By identifying important functional groups on the IR spectrum we can confirm that vanillin was adsorbed. The vibration at 1290 cm^{-1} corresponds to an aromatic C=C stretching vibration. Another aromatic feature, the ring breathing vibration (the ring stretches and contracts symmetrically in all directions) occurs at 1518 cm^{-1} . Aldehyde C-H stretches occur as a doublet at 2804 cm^{-1} and 2840 cm^{-1} . The phenolic O-H stretch occurs at a wide range of $3500\text{-}3300\text{ cm}^{-1}$; although it is difficult to use for kinetic analysis it was identified. The most important and vanillin specific functional group is the aldehydic carbonyl that occurs at 1701 cm^{-1} ; aldehydes usually occur at higher frequencies, but this aromatic aldehyde, which resonates with the conjugated π system, occurs at a significantly lower frequency. This shows that this carbonyl is indeed part of an aromatic system. Combining the aromatic, aldehydic carbonyl and phenolic functional groups vibrations allows us to confirm the presence of vanillin on the KCl surface.

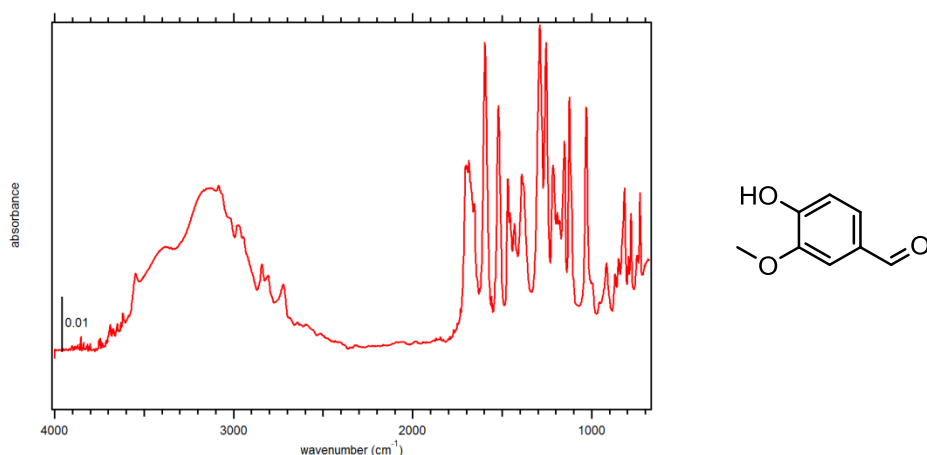


Figure 3.1: IR spectrum of vanillin adsorbed onto KCl substrate collected prior to any ozone or light exposure. Structure of vanillin is shown on the left.

Table 3.1: Important spectral features of vanillin

Wavenumber (cm ⁻¹)	Spectral feature
1518	Aromatic ring breathing
1290	Aromatic C=C stretch
1030	C-O stretch on (near OH)
2840	Aldehyde C-H stretch
2804	Aldehyde C-H stretch
1701	Carbonyl stretch

3.2 Identification of Ozonolysis Products

To understand the impacts of the ozonolysis of vanillin, reaction products were identified via DRIFTS and GC-MS. The light and dark reactions IR spectra are shown below in Figures 3.7 and 3.8. For the light reaction (Figure 3.7) the aldehyde carbonyl peak is no longer easily distinguished.

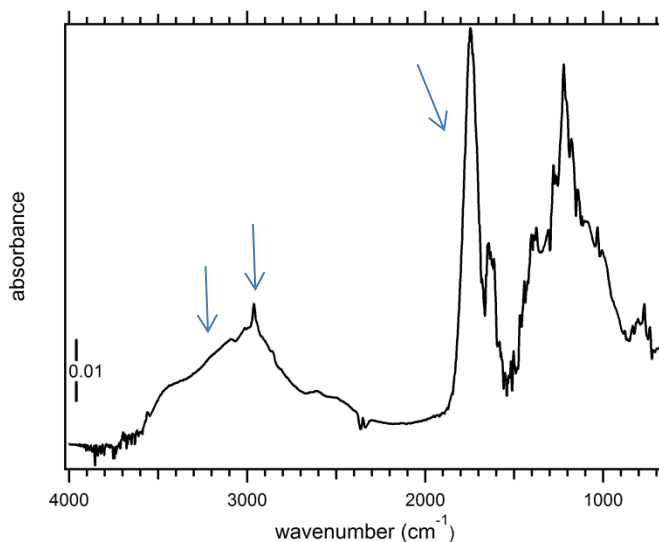


Figure 3.2 : IR spectrum of ozonolysis of vanillin after 800 minutes under light exposure. Arrows indicate the following functional groups from left to right: OH stretch (3200 cm⁻¹), aldehyde CH (2960 cm⁻¹), aldehyde and carboxylic acid carbonyl (1743 cm⁻¹).

In its place is a wider and significantly taller peak that ranges from aldehyde to carboxylic acid carbonyl stretches. It is unlikely that the carbonyl stretches are only from the aldehyde carbonyl on vanillin because the concentration is significantly greater than

the original vanillin carbonyl peak and thus is likely a combination of aldehyde and carboxylic acid peaks. The carboxylic acid peaks are likely from the oxidation of the aldehyde; it may also be a result of ring cleavage between the OH and OCH₃. The new aldehyde peaks may be a result of ring cleavage products where oxidation is not between the OH and OCH₃. In addition, there is significant loss of the aromatic C-H above 3000 cm⁻¹. These may indicate that light reaction does indeed cleave the aromatic ring (as well as oxidize the aldehyde).

Additionally the OH peak at about 3200 cm⁻¹ does not change over the course of the reaction, despite the formation of carboxylic acid groups (which will be a source of OH functionality). This is likely caused by a measurable concentration of adsorbed water, because the OH occurs in the same region it is likely that the OH from carboxylic acid is masked by water OH stretches. Because the concentration of water is significant enough it will not change despite minor changes in OH concentrations from carboxylic acids on the surface. Adsorbed water is also important in the formation of aldehydes (and carboxylic acids produced from cleavage at sites other than where the OH and OCH₃ moieties are located) for the ring cleaved products. The peak at 2960 cm⁻¹ is an aldehyde CH stretch that grows in over the course of the experiment. This indicates that a new type of aldehyde is formed that is only possible from ring cleavage products.

For the dark reaction, the large carbonyl peak is split into two that one of which occurs at 1743 cm⁻¹ and the other at 1648 cm⁻¹ (the original carbonyl peak at 1701 cm⁻¹ for vanillin is right above the aldehyde and below the carboxylic acid, suggesting that a different type of aldehyde is formed). Some aldehyde features are retained, while new aldehyde and carboxylic acid features are grown in. Aldehydes from ring cleavage

products and carboxylic acids may come from further oxidized aldehydes of the ring cleavage products and the oxidation of vanillin's original aldehyde. There is also some retention of the aromatic C-H stretches above 3000 cm^{-1} which may indicate that not all aromatic rings were cleaved.

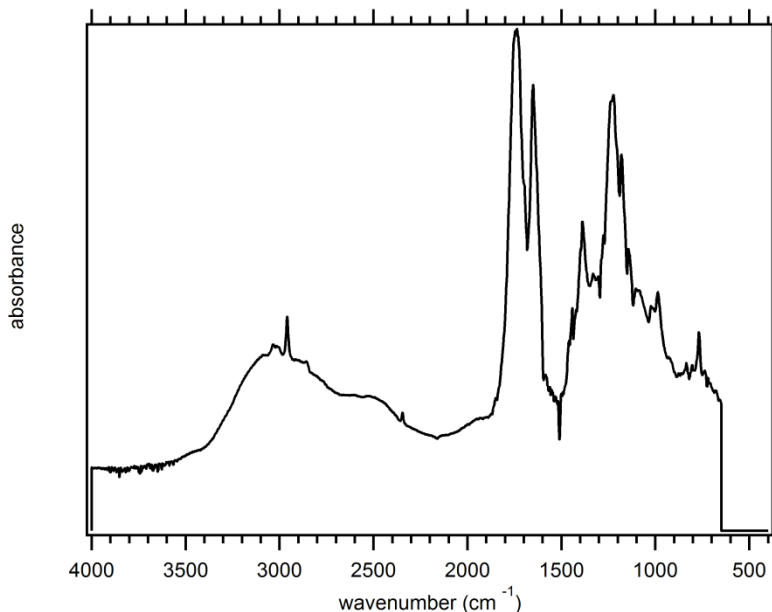


Figure 3.3: IR spectrum of ozonolysis of vanillin after 800 minutes under dark conditions.

Further product identification was conducted via GC-MS. The retention times of vanillin and vanillic acid are 8.9 minutes and 11.25 minutes with molecular ion peaks at 224 and 297 (derivatized), respectively. The GC of light and dark reactions are shown overlapping in figure 3.4 with a major peaks occurring at 11.25 minutes, indicating vanillic acid for both light and dark reactions. The light reaction has a higher abundance of vanillic acid when compared to the dark reaction. There are also numerous signals with significant abundance that may indicate a variety of side products such as potential ring cleavage products that have been further oxidized. Additionally, several contaminants through handling have been identified on the GC chromatograms such as

benzoic acid, sebacic acid, azealic acid, and nonanoic acid (retention times 5.6 min, 12.9 min, 8.7 min, 6.9 min, respectively).

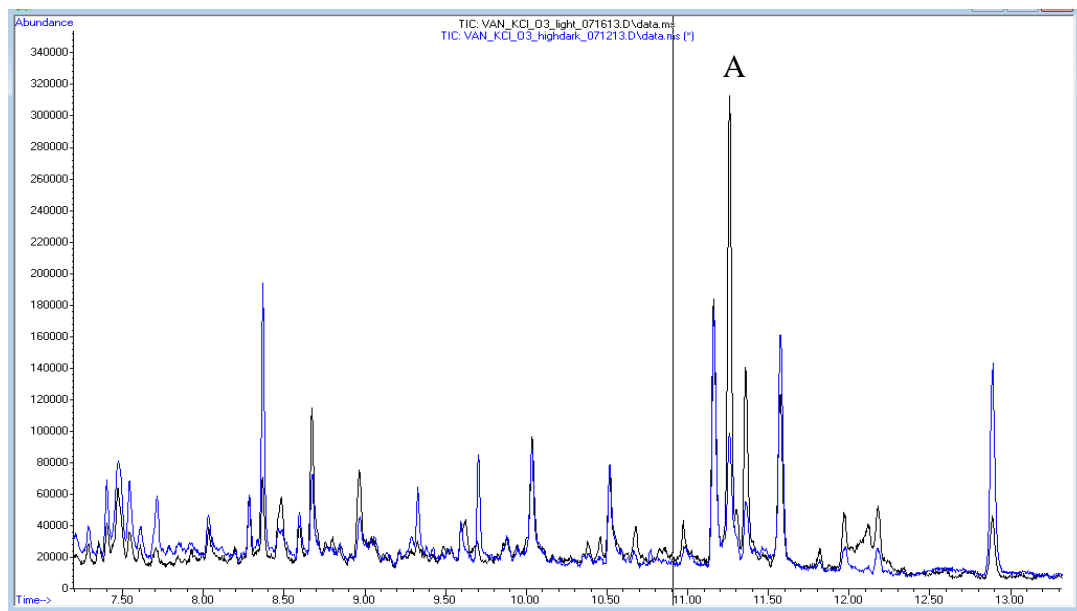
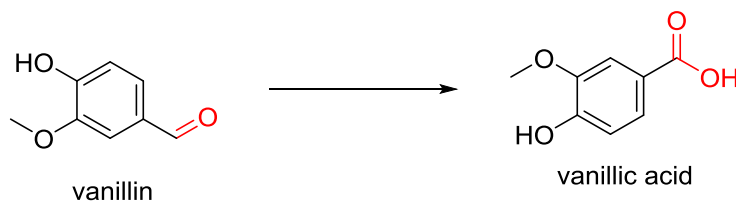


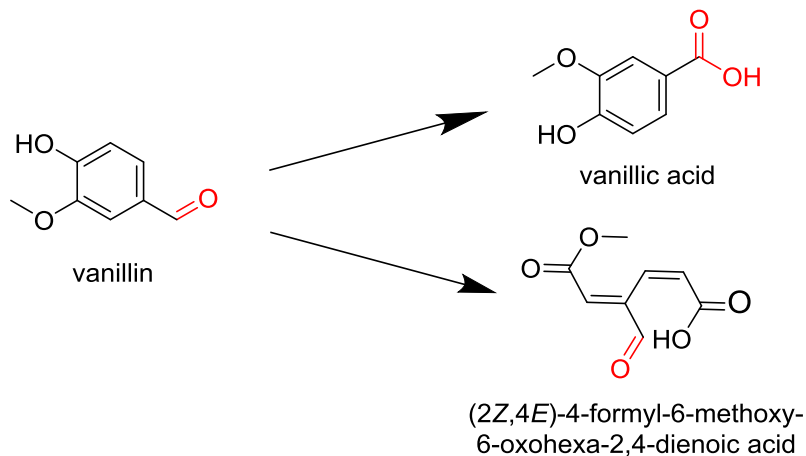
Figure 3.4: GC chromatogram of dark and light reaction products. Blue chromatogram is for dark reaction and black is for light reaction. Peak labeled A is vanillic acid that is present in both light and dark reactions; note concentration differences in light and dark reactions.



S. 3.1

The ring cleavage products were not detected in the GC-MS chromatograms, despite indications in the IR spectra. It is likely that the solvent system (acetonitrile) does not solubilize the ring cleavage products well enough for them to be detected. The structures of the proposed ring cleavage product are shown below. The original aldehyde

of vanillin is in red. Further cleavage of the remaining double bonds may result in new aldehyde moieties and the unidentified products in the GC chromatograms.



S 3.2

3.3 Kinetic Analysis of DRIFTS Data

Figure 3.5 shows DRIFTS reaction spectra as KCl adsorbed vanillin was exposed to O_3 in the light (top) and dark (bottom). Collecting IR spectra overtime allowed us to monitor the changes in peak area. The underlying explanation of how kinetic parameters were obtained is further described below.

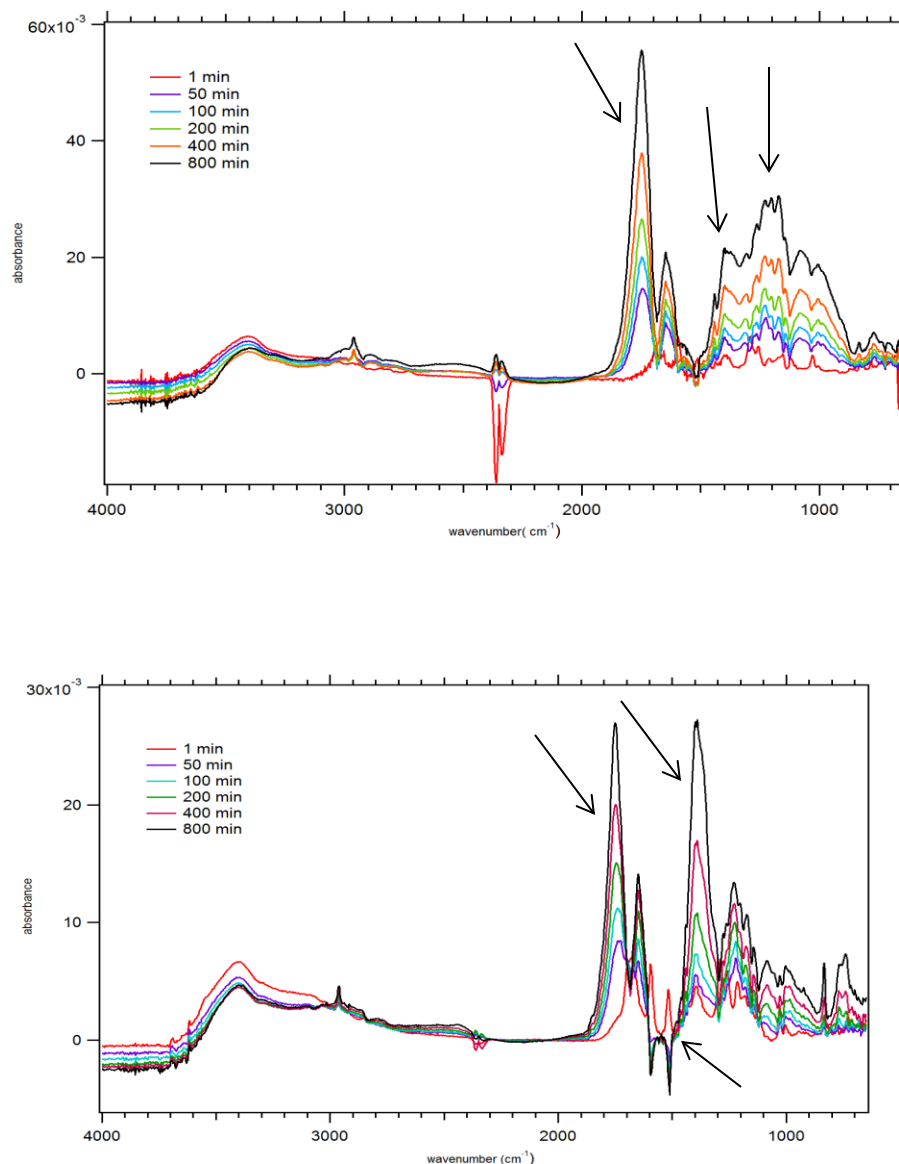


Figure 3.5: (top), (bottom) IR reaction spectra show KCl-adsorbed vanillin at time $t = 0$ and its subsequent reaction with ozone in the presence of light (top) and absence of light (bottom). Important spectral features include the loss of the aromatic feature at 1518 cm^{-1} and the carbonyl growth at 1748 cm^{-1} . Ozone concentrations for light and dark reactions are 7 ppm and 800 ppb.

Generally, the peaks chosen for kinetic analysis included the aromatic ring breathing, aromatic C=C stretch, and the aldehydes C-H stretches at 1518 cm^{-1} , 1290 cm^{-1} , and $2840\text{-}2804 \text{ cm}^{-1}$, respectively. These peaks represented the functionalities that disappear during the course of the reaction at similar rates and were averaged to obtain

the kinetic constants. Oxidation of the aldehyde was highly anticipated because of ozone's strong oxidizing ability. In addition, the aromatic ring was monitored to note any ring cleavage. These peaks were also easily identifiable, distinctive, and did not overlap with neighboring peaks (overlapping peaks are not of a single isolated functional group).

As shown in Figure 3.5, the peak height of certain functional groups decreases while others increase. For example, the aldehyde and aromatic C-H vibrations decrease over the course of the reaction; the most distinctive increase in peak height over the course of the reaction was for the carbonyl peak at 1701 cm^{-1} . The decrease in peak height indicates a decrease in absorbance and a decrease in absorbance is proportional to a decrease in concentration. This relationship is quantified by Beer's Law:

$$\text{Absorbance} = \epsilon * b * c \quad \text{Eq. 3.1}$$

Where ϵ is the molar absorption coefficient, b is the path length, and c is the concentration of the sample. Thus, with decreasing absorption and peak heights, the concentration of specific functional group also decreases. The opposite is also true in which increased peak heights correspond to increased concentrations of a particular functional group.

Absorption peaks were monitored over the course of the experiment; changes in peak area were quantified by integration or calculating area under the curve. The area under the curve was determined by selecting two points at the base of the peak of interest (one to the left and one to the right). The algorithm used then assumed a linear relationship between the two points to find the area under the curve. The area under the curve is proportional to the concentration of surface adsorbed vanillin by Beer's Law.

An illustration of integration is shown below in figure 3.6. The integration of the peaks over the course of the experiment shows how the concentration of the surface adsorbed vanillin changed over the course of the experiment with ozone exposure.

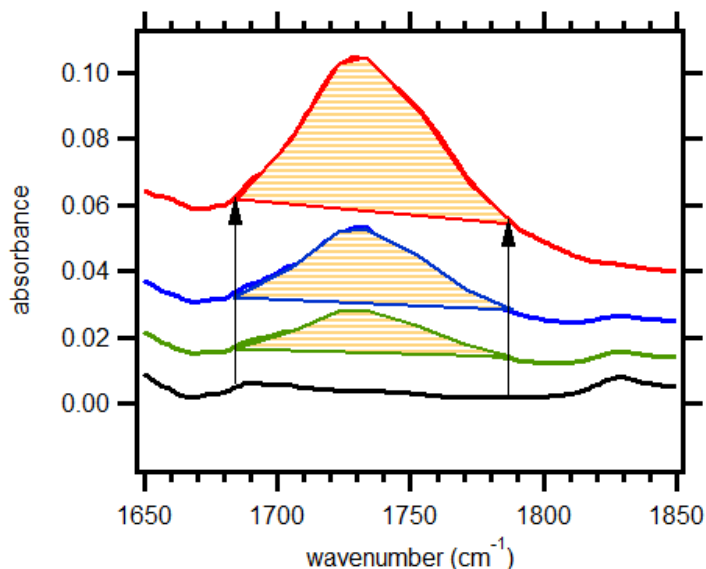


Figure 3.6: Example of integration overtime using eugenol: growth of carbonyl peak at 1743 cm^{-1} for (bottom to top) 1, 35, 50, 90 minutes (black, green, blue, red respectively) in the presence of ozone. Kinetic integrations with sloped baselines (shown by the area under the curves as horizontal orange shading) were studied by selecting endpoints of peaks to integrate, while minimizing overlap with other peaks. The same point on each of the curves was selected when conducting integrations as indicated by the arrows pointing to endpoints of integration and overlap at the same points on subsequent curves. Integrations were used to study the rate of peak growth or disappearance with respect to time. The spectra are offset to illustrate peak growth clearly.

The relationship between the peak heights (concentration of adsorbed organic) and the changes that occur over the course of the experiment is important for the quantifiable kinetic information that we wish to obtain.

3.4 Preliminary Analysis of Photoenhanced Vanillin Ozonolysis

In a single experiment the solar simulator was turned on and off at 15 minute intervals for the first 90 minutes of the reaction. Integrating the product carbonyl peak at 1748 cm^{-1} shows increased rates of ozonolysis under light exposure. This is shown in Figure 3.7 as the linear functions increase in slope under light exposure and decreased slopes in the absence of light. From this we can confirm that rate of the formation of the carbonyl peak is enhanced by the presence of light. The relationship between the light and dark is a 2.5 fold increase rate of ozonolysis in the presence of light. Although this is a preliminary analysis, it does indicate that the reaction is photoenhanced, as one of the functional groups is oxidized faster under simulated solar light.

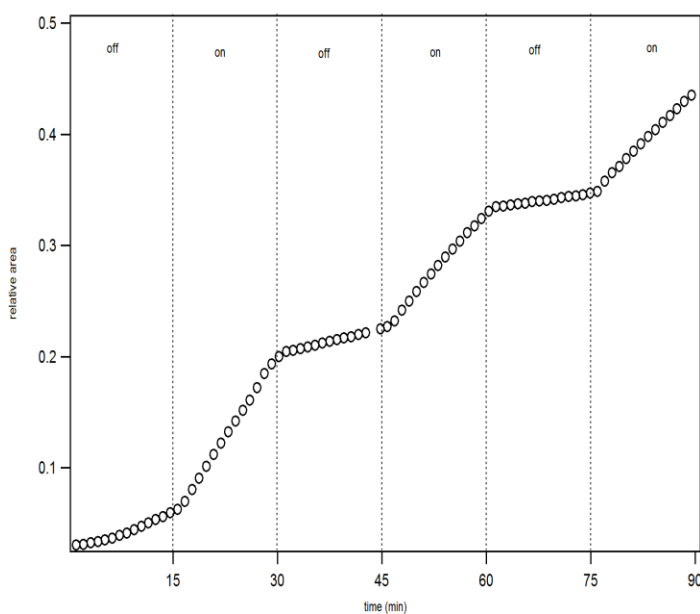


Figure 3.7: Kinetics integration of 1748 cm^{-1} peak with and without exposure to light at 15 minute intervals shows photo-enhancement (single experiment, 269 ppb).

In the experimental procedure, the ozone concentration is held constant because the experiment is conducted under continuous flow. This allows for the simplification of the rate equation to:

$$\text{Rate} = k_{obs}[\text{vanillin}]^n \quad \text{Eq. 3.5}$$

$$k_{(obs)} = k[\text{O}_3] \quad \text{Eq. 3.6}$$

where k_{obs} is the observed rate constant including the ozone concentration which can be experimentally determined.

Experiments were designed to obtain the rates of the reaction involved full course exposure to light or full courses of dark to compare the reaction rates. Using the integration- absorbance theory we were able to quantify how the concentration of specific functional groups changed overtime. For example, the change in area of the 1518 cm^{-1} peak is shown in Figure 3.8 to illustrate how the concentration of that particular peak decreases overtime.

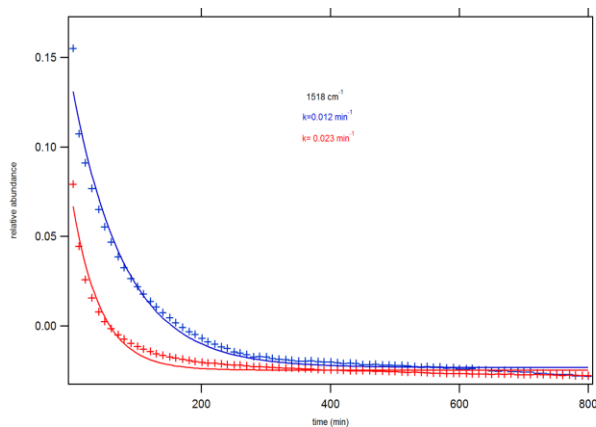


Figure 3.8: Kinetics integration of 1518 cm^{-1} vanillin peak of dark (blue) and light (red) reactions demonstrate the faster decay under exposure to light. Light reaction shown in red (141 ppb) and dark reaction in blue (107 ppb). The decay rate fit (solid curves) of the 1518 cm^{-1} peak in the light is faster than in the dark, indicating photo-enhancement.

The rate of loss of the 1518 cm^{-1} peak was fit to an exponential decay function in the form of:

$$y = y_0 + Ae^{-\frac{(x-x_0)}{\tau}} \quad \text{Eq. 3.7}$$

This was determined by using IGOR Professional, where τ is the decay constant. The inverse decay constant $\frac{1}{\tau}$ is equal to the rate constant k_{obs} . Because the loss of vanillin was fit to exponential decay, this indicates that this reaction is first order with respect to vanillin. Recalling Eq. 3.5:

$$\text{Rate} = k_{obs}[\text{vanillin}]^n \quad \text{Eq. 3.5}$$

Therefore $n=1$ and we can write:

$$\text{Rate} = k_{obs}[\text{vanillin}] \quad \text{Eq. 3.8}$$

Inverse decay constants were used to calculate the k_{obs} for peaks described above. By averaging at least three decay constants we were able to obtain k_{obs} for the oxidation of vanillin. The rate constant, k , can be determined from the decay fit functions of the integrated peaks over time

An important subtlety arises here about the concentration of ozone used. Because this is a heterogeneous system ozone may adsorb onto the surface similar to vanillin or it may remain in the gas phase. There are two possible ways ozone may react with the vanillin: it may be adsorbed onto the surface or may react in the gas phase. We consider two mechanisms that describe each type of reaction, the Eley-Rideal mechanism and the Langmuir-Hinshelwood mechanism.

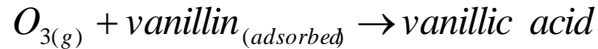
The Eley-Rideal mechanism describes a system in which ozone in the gas phase would oxidize the organic adsorbed onto the KCl substrate. This mechanism predicts that

as ozone concentrations are increased, the k_{obs} would linearly increase, because the reaction is happening at the gas-adsorbed organic on solid interface; this reaction is shown in reaction Scheme 3.1:

$$Rate = k[O_{3(g)}][vanillin]$$

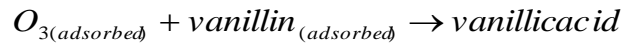
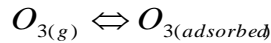
$$k_{(obs)} = k[O_{3(g)}]$$

$$Rate = k_{obs}[vanillin]$$



S 3.1

The Langmuir Hinshelwood model describes a system in which the ozone adsorbs onto the surface of the KCl and then oxidizes the adsorbed organic. This relationship is shown in reaction Scheme 3.2 below:



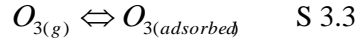
S 3.2

This model is based on the idea that the gas phase molecules are in equilibrium with the solid surface. Here, k_{obs} is linearly proportional to concentration of adsorbed ozone therefore:

$$k_{obs} = k[O_{3(ads)}] \quad \text{Eq. 3.9}$$

The adsorbed ozone concentration however is not known. Our experimental setup is designed to measure ozone concentration in the gas phase not the adsorbed concentration. Thus, we need an expression to relate adsorbed ozone concentration to gas phase ozone

concentration. Recalling that adsorbed and gaseous ozone are in equilibrium we may write:



Where the rate of the forward reaction of adsorption is k_a and the reverse reaction for desorption is k_d , therefore the change in surface coverage θ is:

$$\left(\frac{d\theta}{dt}\right)_{adsorbed} = k_a PN(1 - \theta) \quad \text{Eq. 3.10}$$

$$\left(\frac{d\theta}{dt}\right)_{desorption} = -k_d N\theta \quad \text{Eq. 3.11}$$

Where N is the number of adsorption sites available. The change in the number of occupied sites on the surface is zero therefore:

$$\left(\frac{d\theta}{dt}\right) = 0 = k_a PN(1 - \theta) - k_d N\theta \quad \text{Eq.3.12}$$

The surface coverage at equilibrium is:

$$\theta = \frac{k_a P}{k_a P + k_d} \quad \text{Eq. 3.13}$$

Dividing by k_d yields an expression with K_{O_3} which is the equilibrium constant defined as:

$$K_{O_3} = \frac{k_a}{k_d} \quad \text{Eq. 3.14}$$

The new expression for surface coverage at equilibrium is:

$$\theta = \frac{K_{O_3} P}{1 + K_{O_3} P} \quad \text{Eq. 3.15}$$

Multiplying the number of sites by θ yields the concentration of adsorbed ozone. So that:

$$[O_{3(ad)}] = N_{sites} \theta = \frac{K_{O_3} [O_{3(g)}]}{1 + K_{O_3} [O_{3(g)}]} \quad \text{Eq. 3.16}$$

Recalling that:

$$k_{obs} = k[O_{3(ad)}] \quad \text{Eq. 3.9}$$

Multiplying the right most expression by the rate constant from the adsorbed ozone reaction by k yields:

$$k_{obs} = \frac{K_{O_3} k [O_{3(g)}]}{1 + K_{O_3} [O_{3(g)}]} \quad \text{Eq. 3.17}$$

where k is the maximal rate constant that is obtainable for this reaction k_{max} . Thus the Langmuir-Hinshelwood mechanism was modeled by:

$$k_{obs} = \frac{K_{O_3} k_{max} [O_{3(g)}]}{1 + K_{O_3} [O_{3(g)}]} \quad \text{Eq. 3.18}$$

This model allows us to assume that the organic coating of the KCl substrate is a single layer and that the surface is uniform to simplify the study that involves complex adsorbent- gas interactions.

Where k_{obs} is the observed rate constant, K_{O_3} is the equilibrium constant of ozone, $[O_3]$ is the ozone concentration, and k_{max} is the maximum rate constant achievable for this reaction.

3.6 Kinetic analysis is used to determine the mechanism of ozonolysis of vanillin

Using the Langmuir-Hinshelwood equation, the average observed rate constants of the light reactions were compared to those in the dark. The obtained k_{obs} values from experiments with varied ozone concentrations show a non-linear increase followed by a plateau of k_{obs} values at high ozone concentrations, k_{max} (k_{max} varied for light and dark reactions and is discussed below). The maximal rate achieved indicates that rate of the oxidation cannot surpass a certain rate because the rate constant is dependent on the number of sites available for ozone adsorption. The surface was occupied with vanillin and then saturated with ozone; this defines the Langmuir- Hinshelwood mechanism. For the light and dark reactions, we can conclude that the mechanism of the ozonolysis of vanillin was determined to follow the Langmuir- Hinshelwood model as opposed to the Eley-Rideal mechanism (see Figure 3.9).

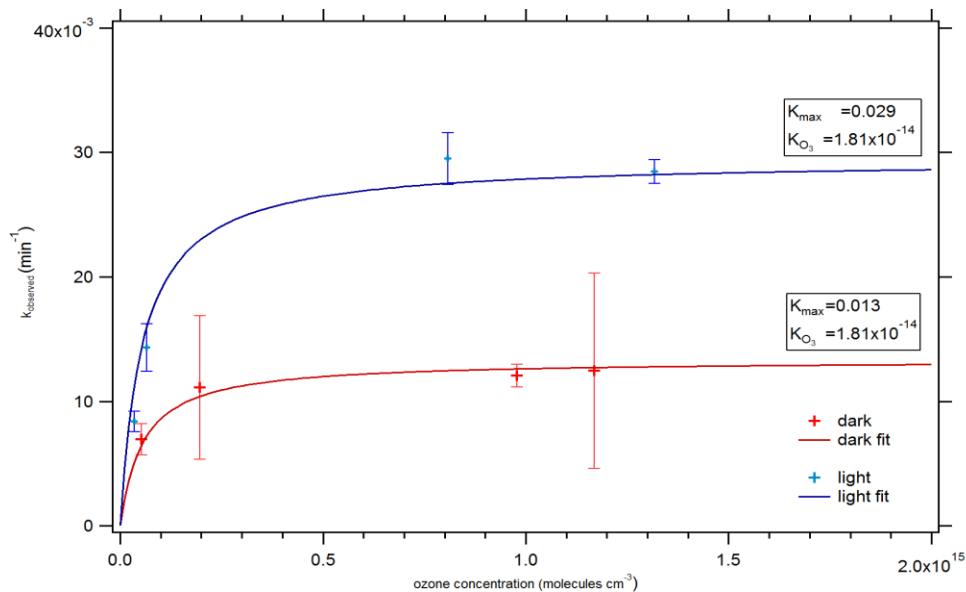


Figure 3.9: Langmuir-Hinshelwood plot of dark (red) and light (blue) reactions of vanillin with ozone. Solid lines indicate curve fits. Each point on the curve represents a single experiment, with averaged and inverse decay constants to obtain k_{obs} values. k_{max} of light reaction approximately double of dark; k_{max} of light reaction approximately double of dark in units of min^{-1} and K_{O_3} is in units of cm^3

In the case of Eley-Rideal mechanism, a k_{max} could not be obtained because the reaction happens at the solid-gas interface in which vanillin reacts with ozone in the gas phase. This type of mechanism is independent of the number of adsorption sites of ozone and will increase linearly with increased ozone concentration. Thus, this mechanism does not describe the reaction of vanillin adsorbed onto the KCl substrate with ozone.

As the ozone concentration increases, the k_{max} reaches a value of 0.029 min^{-1} and 0.013 min^{-1} for the light and dark reactions respectively. The maximal rate constant in the light is over two times the maximal rate constant in the dark. The photo-enhancement of aromatic carbonyls is consistent with other laboratory models. The ozone equilibrium constant K_{O_3} was determined to be $1.81 \times 10^{-14} \text{ cm}^3$ from the non-linear- least squares- fit function to equation 3c based on the Langmuir-Hinshelwood model. K_{O_3} values from similar models in literature occur on the same order of magnitude at $4.5 \times 10^{-14} \text{ cm}^3$ on silica particles (Net et al., 2009).

The atmospheric lifetime of adsorbed vanillin on a KCl substrate can be calculated using the obtained parameters from the Langmuir-Hinshelwood fits and known ozone concentrations of 40 ppb (Vingarzan, 2004). The inverse Langmuir-Hinshelwood was used to calculate the atmospheric lifetime of vanillin in the dark and light. The atmospheric lifetime of vanillin for the dark and light are 8.5 hours and 3.8 hours.

The mechanism of reaction on the substrate indicates the importance of the multiphase chemistry on the surface of aerosols and the differences associated, which in this case are described by the Langmuir-Hinshelwood mechanism. In addition, the presence of light has a significant impact on the atmospheric lifetime of the KCl- vanillin aerosol. This model can be used to estimate the lifetime of similar compounds while considering the effects of light, in this case where light does in fact enhance the rate of oxidation of vanillin by over a factor of 2. This model will provide insight into the mechanistic and kinetic chemistry that is needed to decrease the uncertainty associated with aerosols in the atmosphere.

Chapter 4: Eugenol Reactions: Results and Discussion

The ozonolysis of eugenol adsorbed on a KCl substrate in the presence and absence of light was studied. An IR spectrum of adsorbed eugenol prior to any reaction is shown in Figure 4.1a. Preliminary kinetic analysis was conducted to provide a general understanding of the kinetics prior to detailed analysis. In order to assess the rate of decay of eugenol, several important functional groups of eugenol were identified. Important functional groups that confirm the adsorption of eugenol include the aromatic C-H stretches at 3006 cm^{-1} ; the alkene side chain C=C stretch occurs at 1640 cm^{-1} . The C-H stretches of the alkene side chain occur at 3083 cm^{-1} and 3058 cm^{-1} . These functional groups are shown below in table 4.1. These functional groups were used in kinetic analysis to determine rate constants.

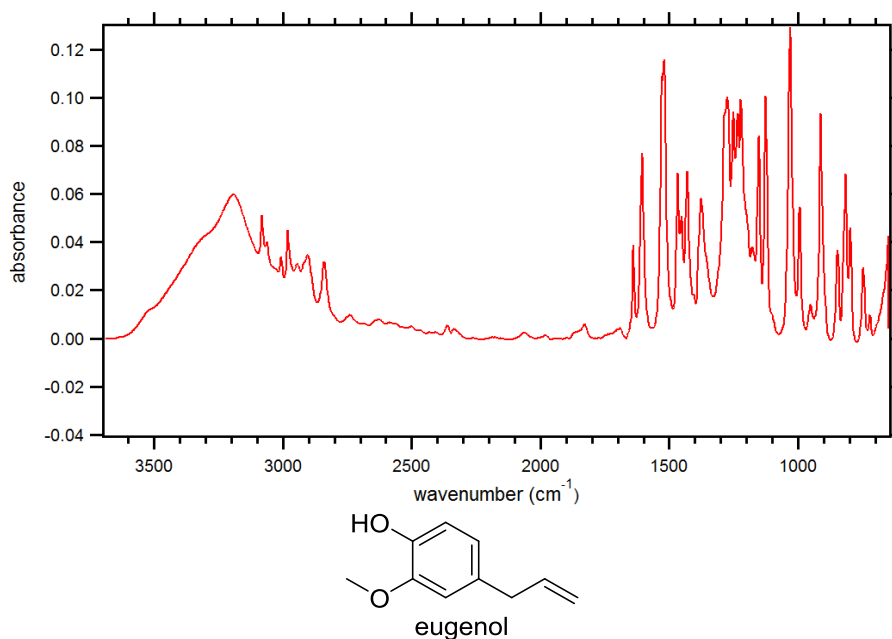


Figure 4.1a . IR spectrum of adsorbed eugenol on KCl surface and structure of eugenol. Several peaks of interest specific to eugenol are labeled directly on the spectrum and will be monitored throughout the experiment Structure of eugenol and likely interactions involved in eugenol adsorption (right).

4.1 Preliminary analysis

An experiment was first conducted to note if the presence or absence of light did have an effect on the rate of the reaction. This experiment was divided into intervals (~20 minutes) of light exposure and no light exposure. The functional groups' rate of decay were monitored and analyzed to take note of any effects. The experiment was conducted at an ozone concentration of 495 ppb. It is important to note that the ozone concentrations in Figures 4.1 and 4.2 were not yet stabilized and is increasing in the first twenty minutes of the reaction. A list of important functional groups is shown below. Integration curves of individual functional groups show different patterns upon exposure and no exposure to light.

Table 4.1. Adsorbed eugenol vibrational modes monitored over the course of reaction with ozone.

Peak of interest	Vibration motion	Wavenumber (cm ⁻¹)
Ph- O-H	bend	1377
Side chain C=C-C-H	stretch	3083, 3058
Side chain C=C	stretch	1640
Aromatic C=C	stretch	1467
Aromatic C-H	stretch	3006
Aromatic C=C	ring breathing	1519
Aromatic C-H	bend	746

The rate of the loss of the alkene side chain of eugenol was studied by monitoring two peaks at 3082⁻¹ and 1640 cm⁻¹ which are the vibrations of the C-H stretch and the C=C stretch respectively shown in figures 4.1 and 4.2.

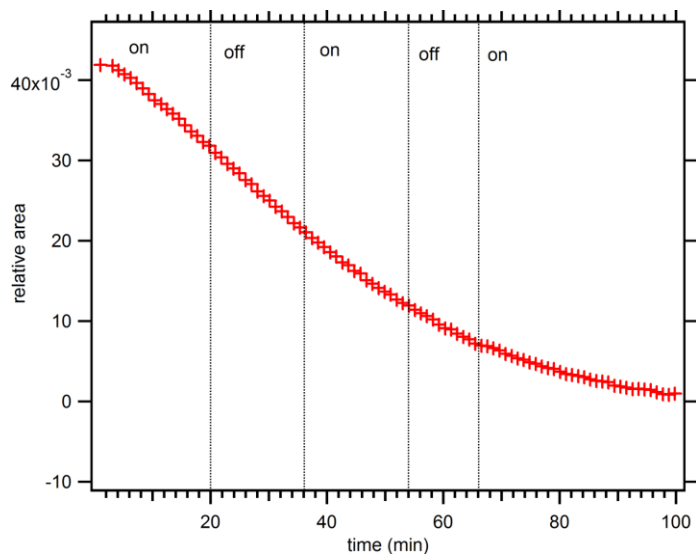


Figure 4.1: Kinetics integration of the 3082 cm^{-1} C-H stretching vibration for alkene side chain. On and off indicate exposure and no exposure to light throughout the course of the experiment. Decay rate is independent of the presence of light as a constant decrease is shown in throughout the experiment. The decay constant is from the exponential decay fit is 443.27 which is used to determine rate constant. Continuous line shows fit function; markers indicate actual data.

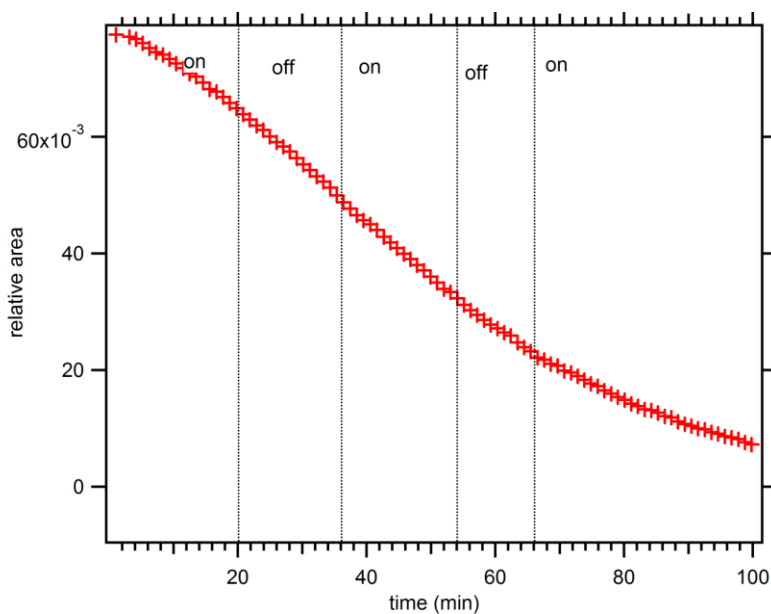


Figure 4.2: Kinetics integration of the 1640 peak; this is the alkene side chain C=C stretching vibration. On and off indicate exposure and no exposure to light throughout the course of the experiment. Decay rate from exponential decay fit is 58.778 and is used to determine rate constant. Continuous line shows fit function; markers indicate actual data.

Upon alternating the exposure to light between on and off, the rate of decay of the peak at 1640 cm^{-1} is not affected by the presence or absence of light. The rate of decay is maintained throughout the experiment and is not altered by light exposure indicating that the ozonolysis of the alkene side chain is independent of the presence of light. Thus, for the alkene side chain, there is no change in the rate of ozonolysis due to light; the constant rate of decay is calculated by the inverse of the rate constant as described above and averaging the values.

The carbonyl peak at 1749 cm^{-1} was monitored and showed different rates of growth in the presence and absence of light. The rate of growth of the carbonyl in the presence of light (and absence of light) was averaged to obtain a relative ratio of the formation of the carbonyl in the light and dark (see figure 4.3).

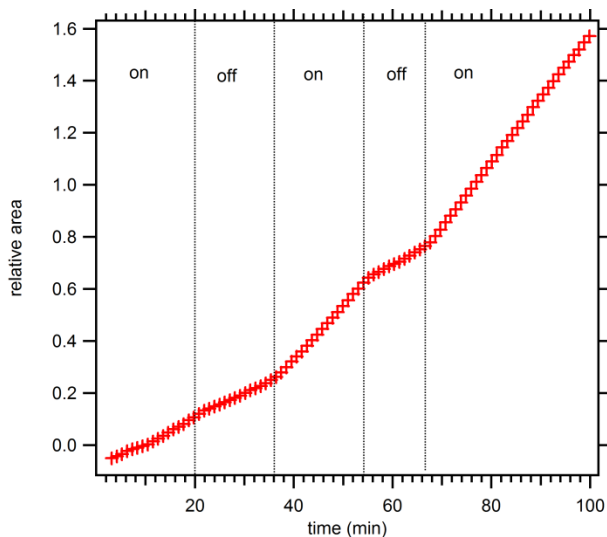


Figure 4.3: Kinetic integration of 1749 cm^{-1} peak (carbonyl stretch) over the course of a light on/ off experiment shows different rates of growth in the presence and absence of light. The rate of the formation of carbonyl is approximately 2.5 times faster in the light than in the dark reactions.

The rate of the light reaction is approximately 2.5 times faster than the rate of the dark reaction for the formation of the carbonyl. It is important to note that the formation of this carbonyl is not solely due to the oxidation of the alkene side chain and is the result of the formation of another carbonyl from the cleavage of the aromatic ring. The photo-enhancement of aromatic features is also shown in Figures 4.4-5; the aromatic C-H stretch at 3007 cm^{-1} shows that the presence of light does enhance the rate of loss of C-H stretches. In addition the methoxy C-H stretch at 1467 cm^{-1} also shows decay and photo-enhancement, which shows that the methoxy feature of the ring is also lost upon exposure to ozone. This indicates that the decay or rate of loss of aromatic ring features is photo-enhanced. It is important to note that the loss of the aromatic features occur at the beginning of the reaction (no delay in loss of features which indicates that the oxidation of the ring is independent of the oxidation of the side chain).

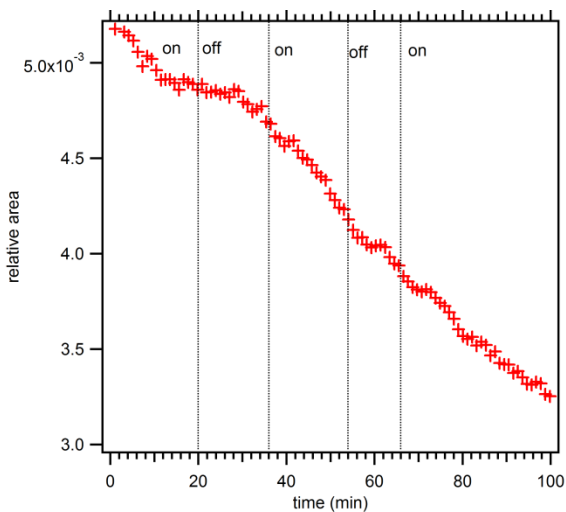


Figure 4.4: Kinetic integration of the 1467 cm^{-1} peak for methoxy CH stretch shows the varied decay rates in the presence and absence of light (ozone concentration 495 ppb). Methoxy C-H stretches are also affected by the presence of light.

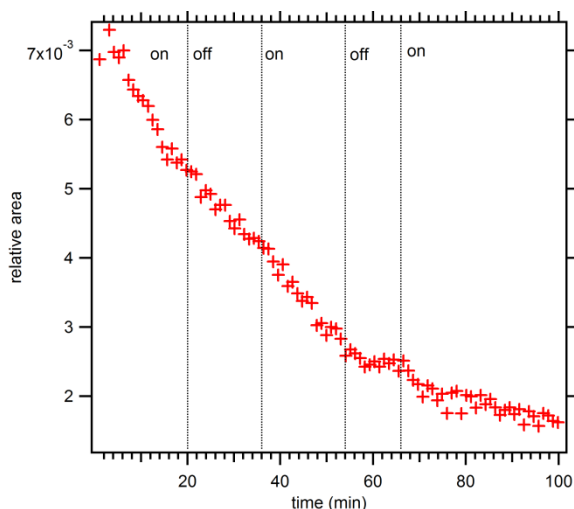


Figure 4.5: Kinetic integration of the aromatic ring C-H stretch vibration at 3007 cm^{-1} shows varied rates of decay when exposed and not exposed to light (ozone concentration 495 ppb). This indicates that the loss of aromatic features do depend on the presence of light.

4.2 A deeper look into eugenol ozonolysis kinetics

Kinetic data from preliminary analysis has shown that the rate of ozonolysis of eugenol, depending on the functional group, demonstrates dependence on the presence of light. The alkene side chain ozonolysis is independent of the exposure to light while the cleavage of the aromatic ring does depend on the presence of light. In order to fully assess and quantify the dependence on light, separate experiments were conducted in which the whole experiment was conducted in the dark or light.

The rate constants (experimental $k_{observed}$ values) of the light and dark reactions of eugenol are shown in figure 4.6 which show a linear relationship. As the ozone concentration is increased the pseudo- first order rate constant increases linearly. The light reaction is approximately 1.1 times faster than the dark reaction.

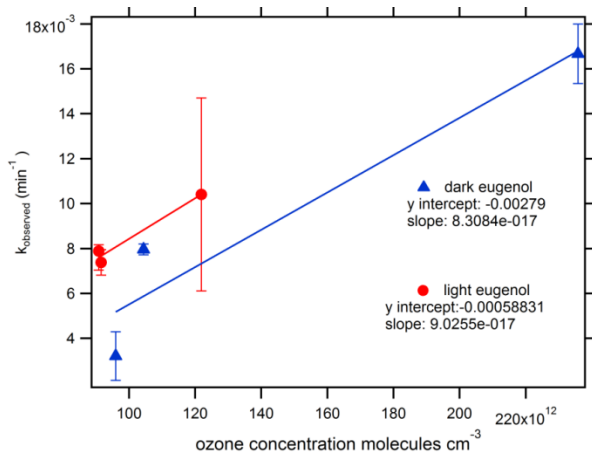


Figure 4.6: linear fit of k_{obs} from kinetic data from adsorbed eugenol reaction with ozone in the light and dark. Light reaction shows increased values of k_{obs} relative to dark reaction.

The relationship between ozone concentration and observed pseudo-first order rate constant gives a partial image into the mechanism of oxidation. Because this reaction proceeds between an adsorbed (eugenol) and gas phase (ozone) species, it is important to consider their interactions with the KCl substrate. In other words, it is important to determine the role of the substrate- essentially clarifying the role of heterogeneous chemistry in this case.

There are two major mechanisms that the oxidation of eugenol can occur by: the Langmuir-Hinshelwood mechanism and the Eley-Rideal mechanism. In the Eley-Rideal type mechanism, gas phase ozone would oxidize adsorbed eugenol at the KCl surface and produce products by oxidation of protruding eugenol molecules. This type of relationship would show a linear relationship of observed pseudo-first order rate constants and ozone concentration. It may seem easy to conclude that the Eley-Rideal mechanism occurs in this case as shown by a linear relationship, but it is important to note the low ozone

concentrations of these experiments. These experiments may indicate the Eley-Rideal Mechanism because only a small section of the full relationship is shown which may mislead us to this conclusion. In addition, based on the structure of adsorbed eugenol, it is difficult to predict any ring cleavage products because the only oxidation of the alkene side chain would occur since it is the only part of the molecule that can interact directly with molecule above it in the gas phase and is not restricted by interactions with the substrate. The other mechanism, Langmuir-Hinshelwood may also occur, in which the adsorbed eugenol is oxidized by adsorbed ozone. As ozone reaches the surface, it adsorbs onto unoccupied sites in the KCl substrate. This relationship would demonstrate that extremely high ozone concentrations would show no increase in the observed rate constant. In other words, the reaction would reach a maximal rate constant or k_{max} as ozone would saturate the surface and not permit the rate constant to increase anymore. The Langmuir-Hinshelwood mechanism is known to occur on aerosol surfaces (Kwamena et al., 2007) and is likely the mechanism of action for eugenol. In order to experimentally prove the occurrence of the Langmuir-Hinshelwood mechanism, higher ozone concentrations would be necessary and would allow us to experimentally rule out the Eley-Rideal mechanism. The experimental setup for eugenol did not allow for the measurement of high ozone concentrations and could not be conducted. Thus, we have used the Eley-Rideal rate constants to determine the atmospheric lifetime of surface adsorbed eugenol to be 18.8 hours and 20.4 hours in the light and dark respectively.

4.3 Product Identification via GC-MS and NMR

The ozonolysis of eugenol yielded several different products which include homovanillic acid, vanillin, vanillyl alcohol and vanillic acid with derivatized molecular weight peaks

at 236, 224, 298, 312 respectively. The ozonolysis of vanillin also produced vanillic acid (TMS- from sample) as the major product (molecular weight, 297). Ring cleavage products were not identified in reactions involving the ozonolysis of eugenol from the NMR nor GC-MS. The ring cleavage products were identified from a combination of kinetic analysis (such as the loss of aromatic features) and the ring cleavage shown in the oxidation of 2-methoxy 4-propyl phenol (similar structure to eugenol in which the doubled bond is saturated) according to the NMR

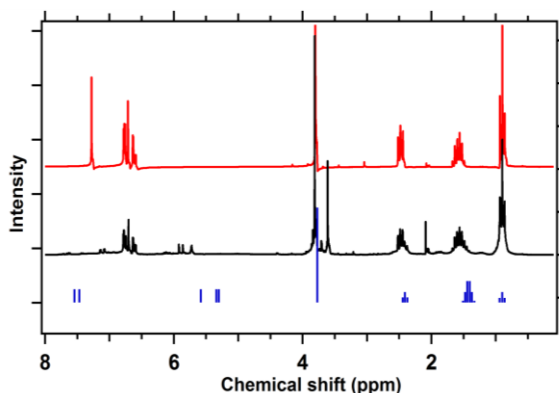


Figure 9. NMR spectra of 2-methoxy-4-propyl phenol prior to reaction with O_3 (red), after reaction with ozone (black), and theoretical prediction (blue). GC-MS identified the MW as 198 g/mol and derivatization using BSTFA confirmed one acid group and a MW of 270 g/mol.

Ring cleavage products of vanillin adsorbed onto silica particles (Net et al., 2011) were not observed likely due to chemisorption of these methoxyphenols onto silica particles. It is important to note that the ring cleavage products do occur in low concentrations and may be difficult to detect, although cannot be ignored.

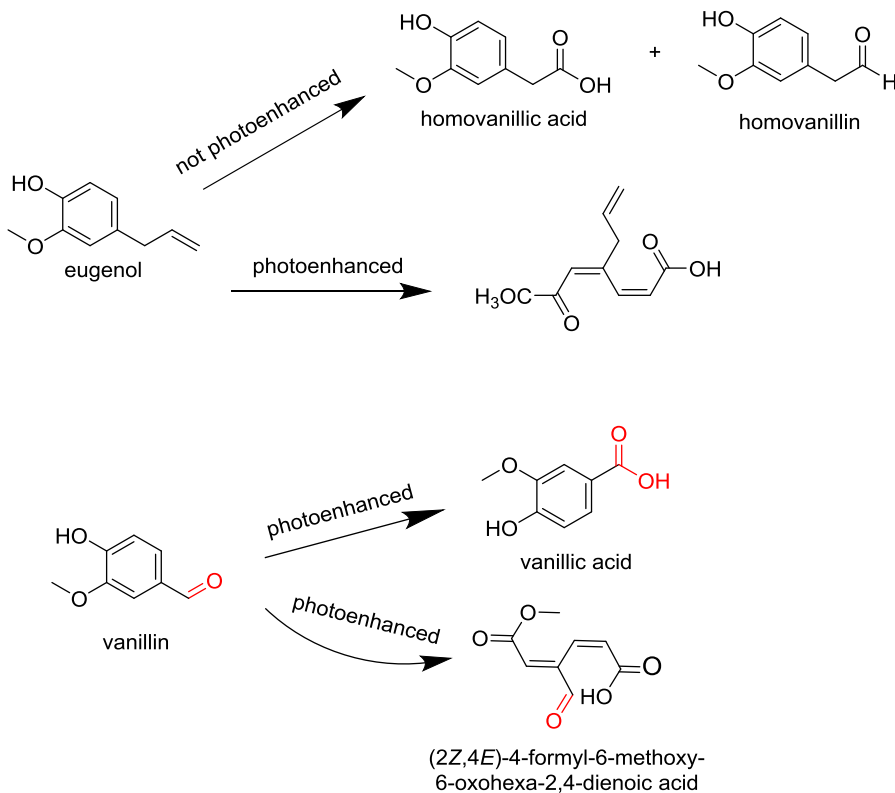
Chapter 5: Importance of Heterogeneous and Photo-enhanced Chemistry in the Troposphere

Understanding the molecular basis of the above reactions will help us understand the molecular processes that drive tropospheric chemistry. It is known that photochemical and heterogeneous processes play a major role in the chemistry of the atmosphere, but the extent of the importance of these processes is generally uncertain when considering biomass burning products. This is especially important when these reactions occur fast enough with other species of the atmosphere to direct chemistry in unexpected manners. Because of the production of numerous compounds from biomass combustion and their ability to react in variable ways, studying these compounds' reactivity necessitates simple laboratory models such as the ones designed here.

As shown in this study, the effects of light have a considerable impact on the rate of reactivity of the model lignin pyrolysis products with ozone. Because the reactions of vanillin and eugenol demonstrate photo-sensitivity, these reactions will be more significant in the day time than in the night. In addition, heterogeneous chemistry is likely to occur at faster rates than gas-phase chemistry. The dependence of the rate of oxidation on the presence of light also shows that these compounds have the ability to absorb light and thus effects the solar radiation that reaches the Earth and the reflected radiation, or the radiative forcing of the Earth which unquestionably affects the energetics of Earth and the climate.

The heterogeneous photochemistry of eugenol and vanillin demonstrates the importance of laboratory models that are simplified models of atmospheric aerosols.

These experiments have shown that the rate of oxidation of a model lignin pyrolysis product is affected by the presence of light in a complicated manner. The kinetics of the reaction of eugenol is complicated by the fact that the rate of ozonolysis of the alkene side chain varies from the cleavage of the aromatic ring in the presence of light. The alkene side chain oxidation is not affected by light exposure while the oxidation of the aromatic ring is enhanced by light exposure. The same molecule, in this case eugenol, adsorbed onto a surface will have different functional groups that demonstrate different kinetics from light exposure. Eugenol's reaction kinetics is especially important because its photo-sensitive properties were unexpected. Vanillin did have photosensitive properties that demonstrate the importance of photochemical processes. This is summarized in Scheme 5.1 below:



Scheme 5.1

The rates of oxidation, reactivity and lifetimes of these species can be used in atmospheric models that show a holistic view of the chemistry in the atmosphere to understand the processes that drive the reactions in the atmosphere that are distant or directly related to these reactions. Atmospheric models designed with this information will help us understand air quality and climate. The uncertainty of the importance of these reactions is also associated with climatic impacts. Because of the reactivity vanillin and eugenol demonstrate with relatively short lifetimes, these aerosol models are important and should be factored into kinetic models. This is especially true in areas where biomass combustion is prevalent and there is significant sunlight reaching a particular area for extended times, such as summer time. Here, we have shown that the heterogeneous ozonolysis of vanillin and eugenol is photoenhanced and should be considered as a reaction that can be used in atmospheric aerosol modeling and can be used to predict the lifetimes of similarly structured lignin pyrolysis products. The factors that were varied such as simulated sun exposure and the heterogeneous trait should be included in laboratory models when modeling aerosol systems. These findings will help to better model aerosol systems' chemistry, climatic effects, and environmental effects to minimize the uncertainty associated with them. These aerosols also have shorter lifetimes than other aerosols which makes them more significant.

The laboratory model designed has provided insight into the mechanistic chemistry and kinetics of the reactivity of these types of aerosols. In order to complete the image of aerosols' chemistry certain factors such as relative humidity and reactivity with other tropospheric pollutants such as NO_2 should be investigated. The reactivity with other tropospheric pollutants is necessary to fully quantify the atmospheric lifetime

of these aerosols. In addition, the role of these organics in the production of hydroxyl radicals should also be pursued, as many organics may be a significant source of hydroxyl radicals, which are another important oxidative and reactive species in the atmosphere. Relative humidity effects on the growth, reactivity, optical properties, and surface effects should be considered for these types of reactions. Additionally, climatic impacts of these methoxyphenols and their products should be pursued by studying their UV-visible absorption properties. This will reveal more about the impacts of their chemical evolution in the atmosphere.

References

- Adachi K., P. R. Buseck: Internally mixed soot, sulfates, and organic matter in aerosol particles from Mexico City Atmos. Chem. Phys., 8, 6469–6481: 2008
- Alvarez E.G., Wortham H. Strekowsky R. Zetzsch C.: Atmospheric photosensitized heterogeneous and multiphase reaction: from outdoors to indoors. Environmental Science and Technology (46) 1955 1963. 2012
- Bedeck, P.R. M Postal Proc Natl. Acadm. Scie. USA 96 :3396-3403 :1996
- Blacet, F.E.; Photochemistry in the lower atmosphere; Ing. Eng. Chem. 44; 1339-342; 1952
- Bond, T.C. Steerts DG. Nelson SM; 2004. A technology based global inventory of black and organic carbon emissions from combustion; Journal of Geophysical research: Atmospheres (109):14:27
- Catsleman, A.W.; Neutral and charged clusters in the atmosphere: the importance and potential role in heterogeneous catalysis; Geophysical monograph; 26:13-25:1982
- Cicerone, R. J., S. Walters, R. S. Stolarski; Chlorine compounds and stratospheric ozone: 188 (4186); 378-379; 1975
- Duan, F., X. Liu, T. Yu, H. Cachier; Identification and estimate of biomass burning contribution to the urban aerosols organic carbon concentration in Beijing. Atmospheric Env. 38 (2004)1275-1282
- Finalyson-Pitts, B.J. and J. N. Pitts; Chemistry of the upper and Lower atmosphere, theory experiments and applications; Academic Press; 2000
- Garcia-Maraver, A., D. Salvachua, M.J. Martinez, L.F Diaz, M. Zamorano . Analysis of the relationship between the cellulose, hemicelluloses, and lignin content and the thermal behavior of residual biomass from olive trees. Waste management (33) 2245-49 ; 2013
- Hawthorne, S. B., M.S. Krieger, D.J. Miller, M.B Mathaison; 1989; collection and quantitation of methoxylated phenol tracers for atmospheric pollution from residential wood stoves. Env. Scie. And Tech. 23, 1191-96
- Jacob, D.J.; Heterogeneous chemistry and tropospheric ozone; Atmospheric environment. (34)12:14 (2131-2159): 2000.
- Jacobson, M.Z.: strong radiative heating due to the mixing state of black carbon in atmospheric aerosols: Nature (409):2001.
- Kwamena N. O., A.Staikova, M. G., Donaldson, D. J. George, J. P. D Abbatt: Role of the aerosol substrate in the heterogeneous ozonation reactions of surface-bound PAHs, J. Phys. Chem. A, (111) 11050–11058; 2007.

- Ma X., K. von Salzen and J. Li: Modeling sea salt aerosol and its direct and indirect effects on climate: *Atmos. Chem. Phys.*: 8,1311-1327, 2008
- McFiggins, G. J.M.C. Plane, B.J. Allan, L.J. Carpenter, H. Coe, C. O'Dowd; A modeling study of iodine chemistry in the marine boundary layer; *Journal of Geophysical Research*; (105) 14: 371-385; 2000
- Middlebrook, A. M., M. A. Tolbert; Global change instruction program: Stratospheric ozone depletion: University Science Books; 2000
- Molina, M. J.; Heterogeneous chemistry on polar stratospheric clouds; (25)11; 2535-2537; 1991
- Montreal Protocol on substances that deplete the ozone layer ; Environmental Protection Agency, 1987
- Net S., E. Alvarez, S. Gligorovski, H. Wortham; Heterogeneous reactions with methoxyphenols, in presence and absence of light; *Atmos. Env.* 2011 (45) 3007-14
- Net S., S. Alvarez, S. Gliogorovski S. Wortham H. Heterogeneous reactions of ozone with methoxyphenols, in presence and absence of light. *Atmos. Env.* (45) 3007-3014: 2011
- O'Neill E., R. Z. Hinrichs; Production of molecular iodine from the heterogeneous reaction of nitrogen dioxide with solid potassium iodide; *Journal of Geophysical Research*; (116); doi; 10.1029; 2011
- O'Neill E.M, Kawam A.Z, Van Ry D, Hinrichs R.Z, Identification of ring cleaved products from the ozonolysis of methoxyphenols adsorbed on aerosol substrates. *In progress.* 2012
- Oros, D. R. B. T Simoneit: Identification and emission factors of molecular tracers in organic aerosols from biomass burning Part 1. Temperate climate conifers: *Applied Geochemistry* (16) 1513-1544:2001
- Oros, D., B. R. T. Simoneit ; Identification and emission factors of molecular tracers in organic aerosols from biomass burning. Art 1. Temperate climate conifers; *Applied Geochemistry* 16; 15513-1544; 2000.
- Parham, R. A., R.L. Gray; In R. Rowell. The chemistry of solid wood. 1984Am Chem. Soc. Washington DC, 33-56 Chapter 1
- Pennar, J. E. et al, Intergovernmental panel on climate change report; 2013
- Pennar, J. E. et al. Aerosols; Their direct and indirect effects IPCC 1998; 291-348

Perri M., S. Seitzinger, B. J. Turpin: Secondary organic aerosol production from aqueous photooxidation of glycolaldehyde: Laboratory experiments. *Atmos. Env.* 43: 1487–1497: 2009

Pettersen, R. C. 1984. In Rowell the chemistry of solid wood. 1984 Am Chem. Soc. Washington DC, 57-126 Chapter 2

Raff, J. D., Szanyi J., Finlayson-Pitts B. J. et al Thermal and photochemical oxidation of self-assembled monolayers on alumina particles exposed to nitrogen dioxide. *Phys. Chem. Chem. Phys* 2011

Read, K. A., et al. ; Extensive halogen-mediated ozone destruction over the tropical Atlantic Ocean; *Nature*; (453)1232-1235; 2008

Ringuet, E. Leoz-Garziandia, H. Budzinski, E. Villenave, and A. Albinet Particle size distribution of nitrated and oxygenated polycyclic aromatic hydrocarbons (NPAHs and OPAHs) on traffic and suburban sites of a European megacity: Paris (France) *J Atmos. Chem. Phys.*, 12, 8877–8887, 201.

Saiz-Lopez, A., J.M.C. Plane, G. McFiggins, P.I. Williams S. M. Ball, M. Bitter R.L. Jones, C. Hongwei, T. Hoffman; Modeling molecular iodine emissions in a coastal marine environment : The link to new particle formation; *Atmos. Chem. Phys*: (6)883-895;2006

Seinfeld, J. H. and M. Bassett: Effect of the mechanism of gas- to-particle conversion on the evolution of aerosol distributions ; *Geophysical monograph*; 26: 6-12:1982

Simoneit, B. R.T. Biomass burning- a review of organic tracers for smoke from incomplete combustion. *Applied Geochemistry* 17 (2002) 129–162

Skoog, D. A., F.J. Holler, S.R.Crouch; *Principles of Instrumental Analysis*; Brooks/Cole Cengage Learning ; 2007

Somorjai, G. A; The surface science of heterogeneous catalysis: possible applications in atmospheric sciences; *Geophysical monograph*; 26: 88-92:1982

Unusual oxidation of organics at interfaces from the bottom up and atmospheric implications; F. Karagulian, C.W.Dilbeck, B.J. Finalyson –Pitts. 2008. *J. Am. Chem. Soc.* 130, 11272-11273

Vaida V., K. J. Feierabend, N. Rontu, K. Takahashi; Sunlight initiated photochemistry: excited vibrational states of atmospheric chromophores; *International Journal of Photoenergy*; AI: 138091; doi: 10.1155/2008/138091: 2008

Van Ry D., Methodology for GS-MS Analysis of Methoxyphenols and Products of Ozonation Reactions; 2012 and GC/MS Work; 2013

Vingarzan, R. *Atmos. Env.* (38) 3431-3442. 2004

Vione D., V. Maurino, C. Minero, E. Pelizzetti, M. A.J. Harrison, R.I. Olariu, C. Arsene; Photochemical reactions in the tropospheric aqueous phase and on particulate matter. *Chem. Soc. Rev.* (35) 441-453; 2006

Vogt R., R. Sanders, R. Von Glasow, P.J. Crutzen; Iodine chemistry and its role in in halogen activation and ozone loss in the marine boundary layer: A model study; *J. Atmos. Chem.*; (32) 375-395; 1999

Winter, B. and Chylek, P.: Contribution of sea salt aerosol to the planetary clear-sky albedo, *49*(1), 72–79, 1997.

Wise, M. E., K. J. Baustian, M.A. Tolbert and B. J. Finlayson-Pitts, Internally mixed sulfate and organic particles as potential ice nuclei in the tropical tropopause region
Author(s): 107, 15 (2010). 6693-6698 PNAS

Woodill L., Hinrichs R.Z. Heterogeneous reactions of surface-adsorbed catechol with nitrogen dioxide: substrate effects for tropospheric aerosol surrogates. *Phys. Chem. Chem. Phys.* (12):10766-10774: 2010

Xu, Y.; W.Huijan L. Hong, F. Ke: Direct Climatic Effect of Dust Aerosol in the NCAR Community Atmosphere Model Version 3 (CAM3); *Adv in Atmos. Sci.* (27)2: 230-242: 2010.